Advances in Water Resources 109 (2017) 302–319

Contents lists available at ScienceDirect

Advances in Water Resources

journal homepage: www.elsevier.com/locate/advwatres

Geophysical characterisation of the groundwater–surface water interface

P.J. McLachlan[a,*], J.E. Chambers[b], S.S. Uhlemann[b,c], A. Binley[a]

[a] Lancaster Environment Centre, Library Avenue, Lancaster University, Lancaster LA1 4YQ, UK
[b] Geophysical Tomography Team, British Geological Survey, Nottingham NG12 5GG, UK
[c] ETH-Swiss Federal Institute of Technology, Institute of Geophysics, Sonneggstrasse 5, 8092 Zurich, Switzerland

ARTICLE INFO

Keywords:
Groundwater–surface water interactions
Groundwater–surface water interface
Hyporheic zone
Geophysics

ABSTRACT

Interactions between groundwater (GW) and surface water (SW) have important implications for water quantity, water quality, and ecological health. The subsurface region proximal to SW bodies, the GW–SW interface, is crucial as it actively regulates the transfer of nutrients, contaminants, and water between GW systems and SW environments. However, geological, hydrological, and biogeochemical heterogeneity in the GW–SW interface makes it difficult to characterise with direct observations. Over the past two decades geophysics has been increasingly used to characterise spatial and temporal variability throughout the GW–SW interface. Geophysics is a powerful tool in evaluating structural heterogeneity, revealing zones of GW discharge, and monitoring hydrological processes. Geophysics should be used alongside traditional hydrological and biogeochemical methods to provide additional information about the subsurface. Further integration of commonly used geophysical techniques, and adoption of emerging techniques, has the potential to improve understanding of the properties and processes of the GW–SW interface, and ultimately the implications for water quality and environmental health.

1. Introduction

It is widely recognised that groundwater (GW) and surface water (SW) form a continuum and are not isolated components (Winter et al., 1998; Malard et al., 2002; Sophocleous, 2002). GW–SW interactions have significant implications for water quantity, water quality, and health of aquatic ecosystems, at site to catchment scales (Winter et al., 1976; Stanford and Ward, 1993; Findlay, 1995; Boulton et al., 1998, 2010; Buss et al., 2009; Harvey and Gooseff, 2015). For instance, contaminated GW discharge can degrade streams, lakes, deltas and wetlands, and associated habitats; conversely GW discharge may also supply vital nutrients and act as a thermal buffer to maintain ecological function (Power et al., 1999; Brunke and Gonser, 1997; Hayashi and Rosenberry, 2002; Marzadri et al., 2013a, 2013b). Over-abstraction of GW can also result in the redistribution or disappearance of SW resources (Winter et al., 1998), and in coastal regions, the contamination of fresh water aquifers (Ingham et al., 2006).

The transition zone between SW environments and GW systems, the GW–SW interface, is important as it governs the exchange of water, nutrients, and pollutants (Kalbus et al., 2006; Buss et al., 2009; Fleckenstein et al., 2010; Lin et al., 2010; Lansdown et al., 2015). Despite conceptually representing an interface, the term GW–SW interface is commonly used to describe alluvial sediments proximal to SW bodies, e.g. stream beds, lake beds, riparian zones, and flood plains. Therefore, it typically has vertical extents up to several metres and horizontal extents on the order of hundreds of metres. It is important to note that here the term GW–SW interface is not synonymous with the hyporheic zone (HZ). The HZs definition is ambiguous and discipline dependent (Stanford and Ward, 1988; Triska et al., 1989; Tonina and Buffington, 2009; Boulton et al., 2010; Ward, 2016; Hester et al., 2017); however it is perhaps best described as the region of the GW–SW interface that occurs non-continuously in both space and time, and permits the mixing of both GW and SW (e.g. Gooseff, 2010). Therefore it is not as ubiquitous as is commonly assumed and mixing is often limited to narrow zones (Hester et al., 2013, 2017). The physical dimensions of the hyporheic zone are also difficult to define, however, the majority of HZ studies focus on lateral scales of 1–10 m and vertical scales of < 1 m (Ward, 2016).

There are numerous established methods that exist for characterisation of the GW–SW interface (Cook and Herczeg, 2000; Stonestrom and Constantz, 2003; Bridge et al., 2005; Greswell et al., 2005; Kalbus et al., 2006; Rosenberry and LaBaugh, 2008; Fleckenstein et al., 2010). However, despite providing direct measurements, use of piezometers, seepagemeters, and boreholes may be limited by site conditions, environmental protection, or installation costs. In this way information

* Corresponding author.
E-mail addresses: p.mclachlan@outlook.com, p.mclachlan@lancaster.ac.uk (P.J. McLachlan).

http://dx.doi.org/10.1016/j.advwatres.2017.09.016
Received 30 April 2017; Received in revised form 4 August 2017; Accepted 14 September 2017
Available online 21 September 2017

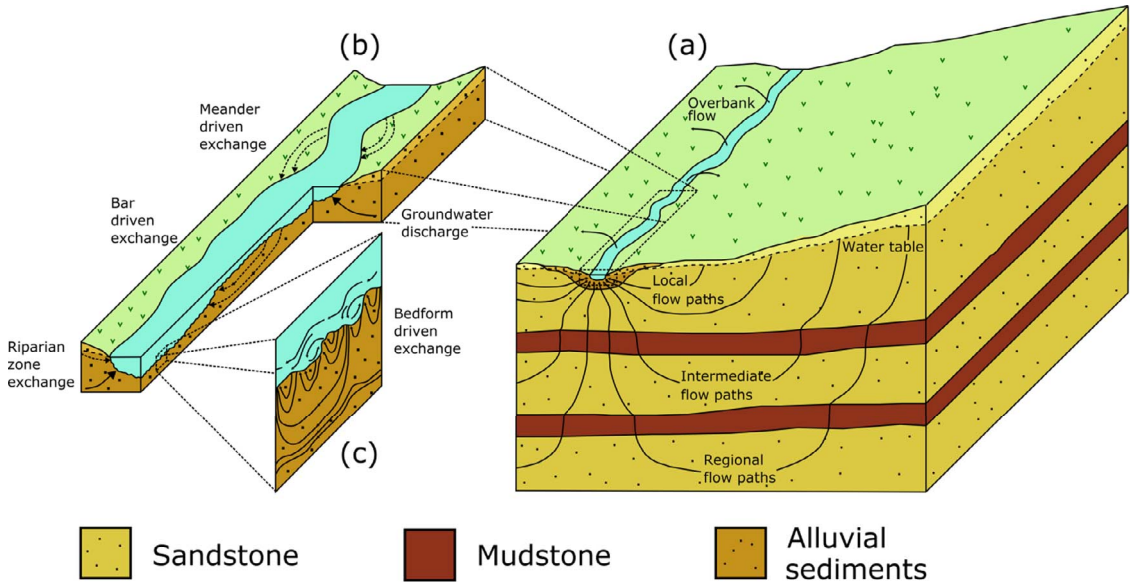

Fig. 1. (a) Various scales of groundwater flow paths and their relation to (b) macro-scale and (c) micro-scale exchanges in a fluvial and floodplain hyporheic zones (after Tóth, 1963; Winter et al., 1998; Stonedahl et al., 2010).

may be spatially limited and unrepresentative. Conversely, tracer experiments (e.g. Findlay et al., 1993; Triska et al., 1993; Harvey et al., 1996; Harvey and Fuller, 1998; González-Pinzón et al., 2015; Xie et al., 2016) provide information that is averaged over larger volumes and therefore may fail to characterise spatial heterogeneity, e.g. identifying low mobility and high mobility zones in the subsurface (Singha et al., 2008).

In the past two decades, near surface geophysics has been increasingly used in characterisation of the GW–SW interface, in addition to other environmental applications (Binley et al., 2015; Parsekian et al., 2015; Singha et al., 2015). Geophysical techniques are sensitive to geophysical properties of the subsurface and hence act as proxies for geological, hydrological, and biogeochemical parameters. It is important to note that while advances in geophysical instruments and subsequent modelling have allowed for more reliable data interpretation, geophysical data can still be ambiguous and often special consideration is required for the deployment of geophysical tools in different settings. Nonetheless, geophysical tools offer the unprecedented opportunity to characterise subsurface parameters at vertical scales of centimetres to hundreds of metres, horizontal scales of metres to hundreds of metres, and temporal resolutions of minutes to hours. Furthermore, given that multidisciplinary research has been essential in GW–SW interface research (Newbold et al., 1982; Bencala, 1984; Valett et al., 1993; Sophocleous, 2002; Wojnar et al., 2013; Ward, 2016), the wider application of geophysical tools would be beneficial. However, it is essential that geophysics is used to address hydrogeological or biochemical problems, rather than hydrogeological or biogeochemical solutions being used to explain geophysical results.

This review focuses on various geophysical tools relevant to characterising properties and processes of the GW–SW interface. In this review, the GW–SW interface and GW–SW interactions are first considered, common geophysical approaches are outlined, various geophysical applications are then reviewed, and finally, avenues of future research are discussed. Although important in governing zones of GW–SW interaction, more general geophysical studies investigating properties of the bedrock aquifers are not included here, but have been the subject of a number of reviews (e.g. Rubin and Hubbard, 2005; Linde et al., 2006; Singha et al., 2007; Holliger, 2008; Hubbard and Linde, 2011; Binley et al., 2015; Singha et al., 2015; Boaga, 2017). However, large scale airborne geophysical studies, which typically sense to depths of tens to hundreds of metres, are considered as they have the potential to provide a large scale context for processes occurring across the GW–SW interface. Moreover, these applications fit well into the requirements of GW–SW interactions to be considered at catchment scales (Kaika, 2003; Hering et al., 2010; Buss et al., 2009; Harvey and Gooseff, 2015).

2. The groundwater–surface water interface

The GW–SW interface is subjected to exchanges spanning multiple spatial scales (Tóth, 1963; Woessner, 2000). At large scales, GW flow paths are principally influenced by hydrostatic forces arising from topography and geology, and occur on scales of metres to hundreds of kilometres (Tóth, 1963; Freeze and Witherspoon, 1967; Winter et al., 1998). On smaller scales, flow paths originating in the SW may temporarily enter the subsurface and allow for GW–SW mixing. These flow paths are commonly referred to as hyporheic exchange flows (HEFs) and are principally governed by geomorphological features (Elliot and Brooks, 1997; Käser et al., 2009; Boano et al., 2014; Hester et al., 2017). HEFs are generally reported to be driven by hydrodynamic forces induced by sand dunes, and cobbles at millimetre to centimetre scales or by hydrostatic forces generated by pool-riffle sequences, sediment bars, meanders, and riparian zones at metres to tens of metres (Harvey et al., 1996; Woessner, 2000; Lautz and Siegel, 2006; Tonina and Buffington, 2007, 2009; Käser et al., 2009, 2013; Stonedahl et al., 2010, 2013; Boano et al., 2014). In this way, hydrological pathways are typically viewed as being nested within in each other (Fig. 1). In reality, this distinction is somewhat arbitrary as HEFs have been stated to occur laterally over hundreds of metres (Boano et al., 2014). Ideally, the point at which the water originating from SW, mixes with and, more closely resembles the GW is the point at which it becomes groundwater recharge regardless of where and when it returns to the surface.

The GW–SW interface is also influenced by temporal variability across scales of milliseconds to years. For instance, turbulent flow in rivers can drive GW–SW mixing within several millimetres of the sediment–water interface on timescales of milliseconds to seconds (Menichino and Hester, 2014; Chandler et al., 2016). On larger timescales, periodic variations in precipitation, snowmelt, evapotranspiration, and flood pulses can modify, or reverse, GW–SW interactions

(Boano et al., 2008; Loheide and Lundquist, 2009; Wondzell et al., 2010; Larsen et al., 2014; Zimmer and Lautz; 2014; Dudley-Southern and Binley, 2015; Malzone et al., 2016; Schmadel et al., 2016). GW–SW interactions can also be influenced by waves and tides (Harvey et al., 1987; King et al., 2009; Bianchin et al., 2011), or driven by density contrasts (Musgrave and Reeburgh, 1982; Webster et al., 1996; Boano et al., 2009).

Properties and processes of the GW–SW interface are therefore highly spatially and temporally heterogeneous. Heterogeneity in alluvial deposits can influence permeability, dispersivity, subsurface residence times, and zones of GW–SW exchange. Also bedrock aquifers can dictate whether interaction are localised (e.g. in fractured or karstic settings) or distributed (e.g. in clastic aquifers), and consequently they influence hydrological and biogeochemical conditions at the GW–SW interface (Nagorski and Moore, 1999; Gandy et al., 2007; Kennedy et al., 2009). Temporal variability in hydrostatic forces can influence locations and timings of GW–SW interactions, the interaction of GW discharge and HEFs, and consequently biogeochemical reactions (Boano et al., 2014). Biogeochemical properties, such as cation exchange capacity, redox gradients, and thermal gradients, have long been known to be important (e.g. Bencala et al., 1984; von Gunten et al., 1991; Winter et al., 1998; Power et al., 1999) but are highly variable, making it difficult to predict pollutant attenuation and nutrient cycling. Furthermore, there have been a limited number of investigations into HZ and GW–SW interface processes across different orders of streams, and their relevance to the catchment (e.g. Gomez-Velez and Harvey, 2014; Kiel and Cardenas, 2014; Marzadri et al., 2017). Therefore, field methods that provide spatially and temporally complete data sets about geological, hydrological, and biogeochemical information at site to catchment scales are required (Buss et al., 2009; Boano et al., 2014; Harvey and Gooseff, 2015; Ward et al., 2016; Hester et al., 2017).

3. Geophysical approaches

The general premise of geophysics is to obtain information about the geophysical properties of the subsurface to infer information about geological, hydrological, and biogeochemical properties (Binley et al., 2015). Geophysical properties can be interpreted using petrophysical models, calibration with other methodologies (both non-geophysical and geophysical), and analysis of temporally distributed data sets of dynamic processes. Geophysical techniques considered here are electrical resistivity (ER), induced polarisation (IP), self-potential (SP), electromagnetic induction (EMI), ground penetrating radar (GPR), and seismic methods (Table 1). Furthermore, forward, inverse, and petrophysical modelling are also briefly discussed due to their importance in data interpretation. Fundamental geophysical theory (e.g. Telford et al., 2010) is beyond the scope of this section, and instead focus is given to the basic principles of field and modelling techniques. Applications of temperature sensing in GW–SW interface studies are also beyond the scope of this review (e.g. Stonestrom and Constantz, 2003; Irvine and Lautz, 2015; Hare et al., 2015; Irvine et al., 2016; Wilson et al., 2016).

3.1. Electrical resistivity

ER methods are used to determine subsurface electrical resistivity by injecting low frequency (< 1 kHz) electrical currents into the ground with two current electrodes and measuring the resultant voltage between two or more potential electrodes (Binley, 2015). ER methods are typically minimally invasive as they commonly involve placing stainless steel electrodes several centimetres into the subsurface, however, in some cases borehole ER is used for enhanced characterisation (e.g. Slater et al., 1997; Crook et al., 2008; Wilkinson et al., 2010; Coscia et al., 2011, 2012). In environmental applications the ER signal is typically dependent on the characteristics of the pore fluid and grain-fluid interface (Glover, 2015). Modern ER instruments are capable of systematically using different combinations of electrodes arranged in lines or grids to image the subsurface in 2D or 3D surveys (Loke et al.,

Table 1
Geophysical techniques and the parameters which they relate to. Rough indications of investigation depths and temporal resolution are also included. In practice, terrestrial surveys typically involve horizontal scales of metres to hundreds of metres, whereas for waterborne and airborne surveys, horizontal extents may be hundreds of metres to tens of kilometres and hundreds of metres to hundreds of kilometres, respectively.

Geophysical technique	Geophysical properties	Examples of derived environmental parameters	Typical investigation depths	Typical acquisition time for 100 m transect
Electrical resistivity	Electrical conductivity	Water content, clay content, pore water conductivity, porosity, stratigraphy	Metres to tens of metres	Tens of minutes
Induced polarisation	Electrical conductivity, chargeability	Water content, clay content, pore water conductivity, surface area, permeability, stratigraphy	Meters to tens of meters	Tens of minutes to hours
Spectral induced polarisation	Electrical conductivity, chargeability (with frequency dependency)	Water content, clay content, pore water conductivity, surface area, permeability, stratigraphy	Meters to tens of metres	Tens of minutes to hours
Self-potential	Electrical potential	Hydrological flux, permeability, redox gradients	Metres	Seconds to minutes
Electromagnetic induction	Electrical conductivity	Water content, clay content, salinity	Metres to Hundreds of Metres	Seconds to minutes
Ground penetrating radar	Dielectric permittivity, electrical conductivity	Water content, porosity, stratigraphy	Metres to tens of metres	Minutes to tens of minutes
Seismic	Bulk density, elastic moduli	Porosity, stratigraphy	Metres to tens of metres	Tens of minutes

2013). These types of surveys are often referred to as ER imaging (ERI) or ER tomography (ERT). In addition to 2D and 3D surveys, temporally distributed measurements can be used to monitor dynamic processes (e.g. Ward et al., 2010a; Johnson et al., 2012; Uhlemann et al., 2016).

3.2. Induced polarisation

IP methods are effectively an extension of ER methods and use low frequency (< 1 kHz) currents to assess the capacitive properties of the subsurface (Binley, 2015). The IP signal typically arises due to the temporary accumulation of ions in porous media following the injection of an electric current (Kemna et al., 2012). Whereas the ER signal is dependent on the properties of both the pore fluid and the porous media, the IP signal is more closely associated with the properties of the grain-fluid interface (Revil et al., 2012). IP can therefore provide information about lithological properties with minimal interference from pore water conductivity (Vinegar and Waxman, 1984; Kemna et al., 2000; Lesmes and Frye 2001; Weller et al., 2013; Glover, 2015). As with ER methods, IP measurements can be made using two current electrodes and two potential electrodes. Modern multichannel systems permit the use of multiple potential dipoles simultaneously in addition to recording the full waveform of the IP signal. Induced polarisation can be conducted in either the time or the frequency domain (Revil et al., 2012). Time domain IP methods involve injecting a direct electrical current between the current electrodes before abruptly switching it off and measuring the voltage decay over a specific time interval between the potential electrodes. Frequency domain IP involves injecting alternating electrical currents and measuring the impedance and the phase lag of the current and voltage waves. Frequency domain IP methods can also be carried out using multiple frequencies to assess the frequency dependent impedance and phase shift between injected current and measured voltage, this is typically referred to as spectral IP (SIP).

3.3. Self-potential

Unlike ER and IP methods, SP methods are passive in that they measure naturally occurring voltages within the subsurface (Jackson, 2015). The SP method is relatively simple in that voltages can be measured using non-polarising electrodes and a high impedance voltmeter (Minsley et al., 2007). Non-polarising electrodes are required to minimise polarisation at the electrode surface and a high impedance voltmeter is required to avoid drawing current from the ground. Under natural conditions the SP signals arise from electro-kinetic, electrochemical and thermo-electric effects (Wynn and Sherwood, 1986; Revil et al., 2012; Jackson, 2015). The electro-kinetic effect, or streaming potential, arises from the advective transfer of excess charges through porous materials (Rizzo et al., 2004). The electro-chemical effect originates from the presence of ion and electron concentration gradients, such as those resulting from redox conditions (Sato and Mooney, 1960; Revil et al., 2010). The thermo-electric effect is caused by the differential thermal diffusion of ions in pore fluid and electrons and donor ions in porous media (Wynn and Sherwood, 1986).

3.4. Electromagnetic induction

Whereas ER, IP, and SP use low frequency (< 1 kHz) electrical currents, electromagnetic methods (e.g. EMI and GPR) use higher frequency signals to induce electromagnetic effects in the subsurface. EMI instruments operate in either the frequency domain (FD-EMI) or the time domain (TD-EMI) and use primary and secondary coils to determine subsurface electrical conductivity and magnetic susceptibility (Everett and Meju, 2005; Fitterman, 2015). In FD-EMI systems a primary current with a specific angular frequency is generated in the primary coil; this induces a primary magnetic field that is out-of-phase with the initial current. The primary magnetic field creates an electromagnetic force that induces eddy currents in the subsurface and a consequent secondary magnetic field. The secondary magnetic field is detected by the secondary coil and is used to infer information about in-phase and out-of-phase components of the subsurface electromagnetic properties. In TD-EMI systems, a current is typically passed around the primary coil before it is abruptly switched off. This current generates a primary magnetic field which induces an electromagnetic force, both of which are in-phase with the primary current. The electromagnetic force generates eddy currents that decay by ohmic dissipation following termination of the primary current. The decay of the eddy currents produces a secondary magnetic field and its rate of change through time is measured by the secondary coil to infer subsurface conductivity (Nabighian and Macnae, 1991). Modern FD-EMI instruments contain multiple secondary coils and can be used to detect information from several depths simultaneously. EMI systems have advantages over electrical methods in that they do not require contact with the subsurface, allowing for easier usage in waterborne or airborne surveys (e.g. Butler et al., 2004; Binley et al., 2013; Harrington et al., 2014).

3.5. Ground penetrating radar

As with EMI, GPR methods use electromagnetic signals to assess subsurface properties. However the frequencies used in GPR are higher (10 MHz to 2 GHz), such that the signal travels by wave propagation, rather than by diffusion. In GPR systems a high frequency signal is emitted into the subsurface via a transmitter antenna before it travels to the receiver antenna, e.g. by reflection from an interface of contrasting electrical properties (Huisman et al., 2003; Annan, 2005; van der Kruk, 2015). The amplitudes and travel times of the returning waves are then used to determine dielectric properties and locate boundaries in the subsurface. Field studies often involve time domain GPR systems and typically use frequencies between 50 and 500 MHz. Frequency domain systems are also available, and in some cases using wider bandwidth permits more accurate modelling of the subsurface (Lambot et al., 2004, 2006). The depth of penetration of the signal is dependent upon the electrical conductivity of the subsurface and the frequencies used. Due to frequency dependent attenuation mechanisms, higher frequencies do not penetrate to as great depths but permit higher resolution images. Furthermore, highly electrically conductive environments may attenuate the signal and reduce the penetration depth.

3.6. Seismic methods

Seismic methods operate in a similar way to GPR but use the propagation of acoustic energy to infer information about the mechanical properties of the subsurface (Steeples, 2005; Schmitt, 2015). Seismic surveys can be conducted by generating waves with an acoustic source (e.g. a sledgehammer). When these waves reach boundaries of contrasting mechanical properties, some energy may refract along the boundary before returning to the surface. Returning seismic waves are detected by a series of receivers (geophones) on the surface and can be used to calculate seismic wave velocity, mechanical impedance, elastic moduli, and determine the locations of structural boundaries.

3.7. Geophysical modelling

Forward modelling is used to calculate the data that would theoretically be observed for a given distribution of geophysical properties. The underlying principles of geophysical methods are well understood, so the creation of synthetic data sets from a model of geophysical properties is straight forward (Binley, 2015). Forward modelling serves two key purposes: (1) to aid survey design and (2) to assist in inversion and interpretation of data. For instance, different geophysical methods and measurement schemes have different strengths and weaknesses. Therefore, by making reasonable estimates of the subsurface properties,

the usefulness of a geophysical technique can be assessed prior to its deployment (Terry et al., 2017). Forward modelling may also be useful in guiding interpretation of unusual features, and prior to sufficient computational power, geophysical data was often interpreted by comparing data with forward models, such as ER sounding curves (Loke et al., 2013).

Inverse modelling is the process of determining the distribution of subsurface geophysical properties based on observed geophysical data and any prior information. The principles of geophysical inversion are beyond the scope of this paper but information can be found elsewhere (e.g. Aster et al., 2005; Tarantola, 2005; Menke, 2012; Linde et al., 2015). The majority of inverse problems are non-unique in that there can be an infinite number of solutions for one geophysical data set. In order to constrain the inversions, regularisation may be used to introduce assumptions to prevent over fitting of data and encourage unique solutions, e.g. lateral smoothing in stratified deposits (Constable et al., 1987; Tarantola, 2005). Moreover, uncertainty can further be reduced by carrying out joint or coupled inversions. In hydrogeophysics, joint inversions involve incorporation of various geophysical and hydrogeological data sets (e.g. Linde et al., 2006; Herckenrath et al., 2013) while coupled inversions model geophysical data within the bounds of prior hydrological models (e.g. Hinnell et al., 2010; Huisman et al., 2010).

In order to be of use in hydrogeology, geophysical models are often interpreted in terms of geological, hydrological, or biogeochemical parameters. Although geophysical data can be interpreted qualitatively (e.g. by locating contrasts in geophysical properties), by monitoring dynamic processes (Johnson et al., 2012; Singha et al., 2015), or through combination with other methods (e.g. Day-Lewis and Lane, 2004; Moysey et al., 2005; Huisman et al., 2010; Miller et al., 2014), petrophysical relationships are commonly used. Petrophysical relations can be used in joint inversions to relate two independent geophysical methods (e.g. Hoversten et al., 2006; Zhang and Revil, 2015) or after geophysical inversion to translate geophysical data. Although mechanistic petrophysical models exist (e.g. Leroy and Revil, 2009; Montaron, 2009; Revil et al., 2012), the majority of models used are semi-empirical or empirical. For instance, models have been developed to relate electrical conductivity and porosity (Archie et al., 1942; Waxman and Smits, 1968), to link water content with dielectric permittivity (Topp et al., 1980), and to interpret and IP responses with surface area, grain size, and permeability (Vinegar and Waxman, 1984; Börner and Schön, 1991; Slater and Lesmes, 2002; Binley et al., 2005; Slater et al., 2007; Weller et al., 2013, 2015a, 2015b, 2015c). It is also important to note that electrical conductivity is also linked to temperature, and as a result, ERI monitoring studies are often corrected for temperature (e.g. Brunet et al., 2010; Chambers et al., 2014a; Uhlemann et al., 2016).

4. Geophysical characterisation of groundwater–surface water interactions

Geophysical applications to characterise properties and processes at the GW–SW interface can be split into three principle areas: (1) characterising subsurface structure, (2) mapping zones of GW–SW connectivity, and (3) monitoring hydrological processes. Whereas structural characterisation and GW–SW exchange mapping have included studies at site and catchment scales, monitoring dynamic processes has been conducted solely at site scales. In this section various geophysical applications relevant to characterising the GW–SW interface are discussed. The majority of studies have focused on freshwater streams and rivers; however, studies have also been conducted in wetlands, deltas, and lakes.

4.1. Structural characterisation

Structural characterisation is essential as the structure governs hydrological properties and subsequent processes. Although minimally intrusive, calibration of geophysics with intrusive methodologies is often required to interpret geophysical information (e.g. Zhou et al., 2000; Chambers et al., 2014b). Also, in some cases borehole methods involving ERT, IP, GPR, or seismic methods may be used for increased resolution of the deeper subsurface (e.g. Slater et al., 1997; Huisman et al., 2003; Kemna et al., 2004; Crook et al., 2008; Dorn et al., 2011). Nonetheless, geophysical methods provide a level of resolution that would be unachievable through use of point measurements alone.

4.1.1. Small scale structural characterisation

Several applications have used geophysics to characterise subsurface structure at the Hanford Nuclear Site (Washington, US) to assess pollution pathways to the Columbia River (Johnson et al., 2015). For example, Slater et al. (2010) used waterborne ERI and IP surveys to determine the contact depth of a high permeability unit and low permeability sections of the underlying unit. Depressions in the contact interface were interpreted to be palaeochannels, and were shown to be areas of GW discharge by using distributed temperature sensing. Land-based IP surveys were also conducted at the site and were effective in revealing contrasts between the two units and locating palaeochannels (Mwakanyamale et al., 2012). The locations of these palaeochannels were also in agreement with later studies that used temporally distributed ERI to monitor GW–SW interactions (Johnson et al., 2012; Wallin et al., 2013), as discussed in Section 4.3. Also at the Hanford Site, Williams et al. (2012a–d) used seismic surveys over several tens of kilometres to interpolate the sandstone-basalt interface between boreholes. They identified significant lows in the contact and determined additional potential pollution pathways to the Columbia River.

A number of geophysical studies have also been conducted at a riparian wetland (Boxford, UK). Crook et al. (2008) used surface and down borehole ER methods to reveal geological boundaries beneath the neighbouring River Lambourn. In the wetland, Chambers et al. (2014b) used ERI, soil probing and borehole data to characterise the 3D structure of the subsurface. They identified different superficial deposits, determined the depth to the chalk bedrock, and identified the weathering profile within the chalk, all of which are likely to have important hydrological implications (Fig. 2). Loke et al. (2015) compared a standard ERI Wenner array and an optimised array and found that the optimised array was able to locate geological interfaces with greater accuracy. In another study, surface GPR revealed that the gravels subdivide into a lower section of chalky gravels and an upper section of coarse flint gravel (Newell et al., 2015). The study also found that gravels below a depth of 2 m were relatively structureless whereas the shallower gravels displayed potential point bar lateral accretion surfaces in association with the peat channels, which are likely to have further implication for hydrology of the site.

Geophysics has also been employed successfully for site scale structural characterisation in a variety of other settings. Crook et al. (2008) used ERI to evaluate the structure and volume of alluvial deposits in Oregon (US), highlighting how it could be used to provide valuable information to model biogeochemical exchange. In comparison, Mermillod-Blondin et al. (2015) characterised alluvial structure using GPR in the Rhone River (Lyon, France). They identified two lithofacies and installed piezometers to monitor hydraulic head and temperature. Samples were also taken to assess water chemistry, sedimentology, and bacterial and invertebrate assemblages. They found that HEFs were faster in the cobble/gravel facies than the gravel/sand facies, and that faster flow led to a greater delivery of organic carbon and an increase in microbial activity. Revil et al. (2005) demonstrated how ERI can be used to determine the 3D geometry of a palaeochannel and showed that SP can be used to determine preferential flow paths (Camargue, France). Several studies have also indicated how multiple geophysical techniques can be used to more accurately characterise the subsurface structure (e.g. Gallardo and Meju, 2004; Günther and Rucker, 2006; JafarGardomi and Binley, 2013). For instance,

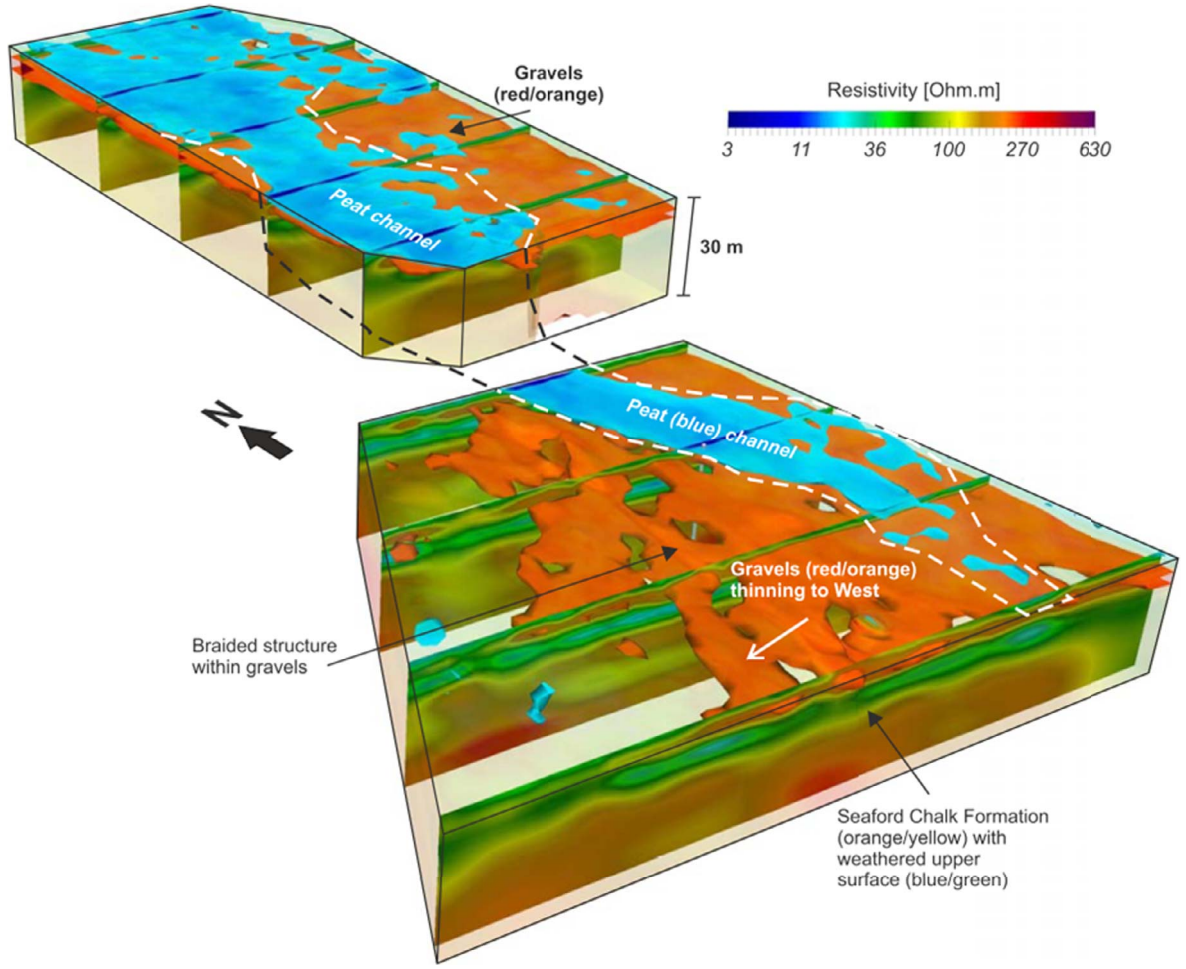

Fig. 2. 3D resistivity model of the Boxford riparian wetland. Solid volumes are shown for regions with resistivities of less than 50 Ohm .m (peat) and with resistivities greater than 150 Ohm .m (gravel) (Chambers et al., 2014b).

Doetsch et al. (2012a) and Zhou et al. (2014) were able to improve structural characterisation at the Thur River, Switzerland by structurally guiding ERI inversion with GPR data. As well as constraining geological boundaries, geophysics has been used to enhance the spatial extent of hydrogeological information. For example, Doro et al. (2013) correlated ERI with slug and pumping tests at the River Steinlach, Germany and Miller et al. (2014) used ERI and permeameters at several alluvial floodplains in Oklahoma, US.

Although the majority of structural studies provide static images of the system, SW systems, particularly rivers, are characterised by dynamic erosional and depositional patterns. This dynamic nature is known to have important hydrological and biogeochemical implications for processes in the GW–SW interface (Elliot and Brooks, 1997; Packman and MacKay, 2003; Harvey et al., 2012). Toran et al. (2012) used ERI to determine changes in sedimentation following installation of a restoration structure, however the dynamic nature of river beds is more widely studied in civil engineering where scouring may lead to undermining of bridge foundations (Anderson et al., 2007). Several methods (e.g. echo sounding, intrusive measurements, bulk electrical conductivity probes) have been used to assess changes in channel bed geometry (Prendergast and Gavin, 2014). However, GPR and seismic methods have been particularly useful as they can provide information about the channel geometry and sediment structure beneath the sediment–water interface without the need for intrusive measurements (Webb et al., 2000; Prendergast and Gavin, 2014).

4.1.2. Large scale structural characterisation

Large scale structural characterisation has typically used airborne TD-EMI (AEM) in association with other data sets. Harrington et al. (2014) used AEM, geological maps, and environmental tracers to infer aquifer architecture beneath a large river in north-western Australia at the catchment scale (Fig. 3). They postulated zones of GW discharge which could be useful in targeting sites for future investigation. AEM has also been used alongside geological mapping data to reveal sedimentary structures and faults (Jørgensen et al., 2012), with ERI to reveal geological variability in deltaic deposits (Meier et al., 2014), with borehole data to identify hydrofacies in glacial deposits (He et al., 2014), with seismic methods to identify the bedrock-superficial interface (Oldenborger et al., 2016), and with modelling to aid in predicting nitrate reduction at catchment scales (Refsgaard et al., 2014). Although AEM dominates regional scale geophysical surveys, other techniques have also been used. Froese et al. (2005) used ERI and GPR at 20–40 km intervals, along with lithological descriptions of bank cuttings to characterise alluvial deposits along a 1000 km reach of the Yukon River (N. America), and Ball et al. (2006) used waterborne ERI and geological borehole data to characterise leakage potential in the Interstate and Tristate Canals (US). Columbero et al. (2014) also used waterborne ERI surveys to characterise the subsurface structure of a glacial lake (NW Italy). They identified an area where lacustrine silts had reduced thickness, and found that this region coincided with anomalous SP signals. They tentatively suggested that SP could be used to locate zones of GW discharge.

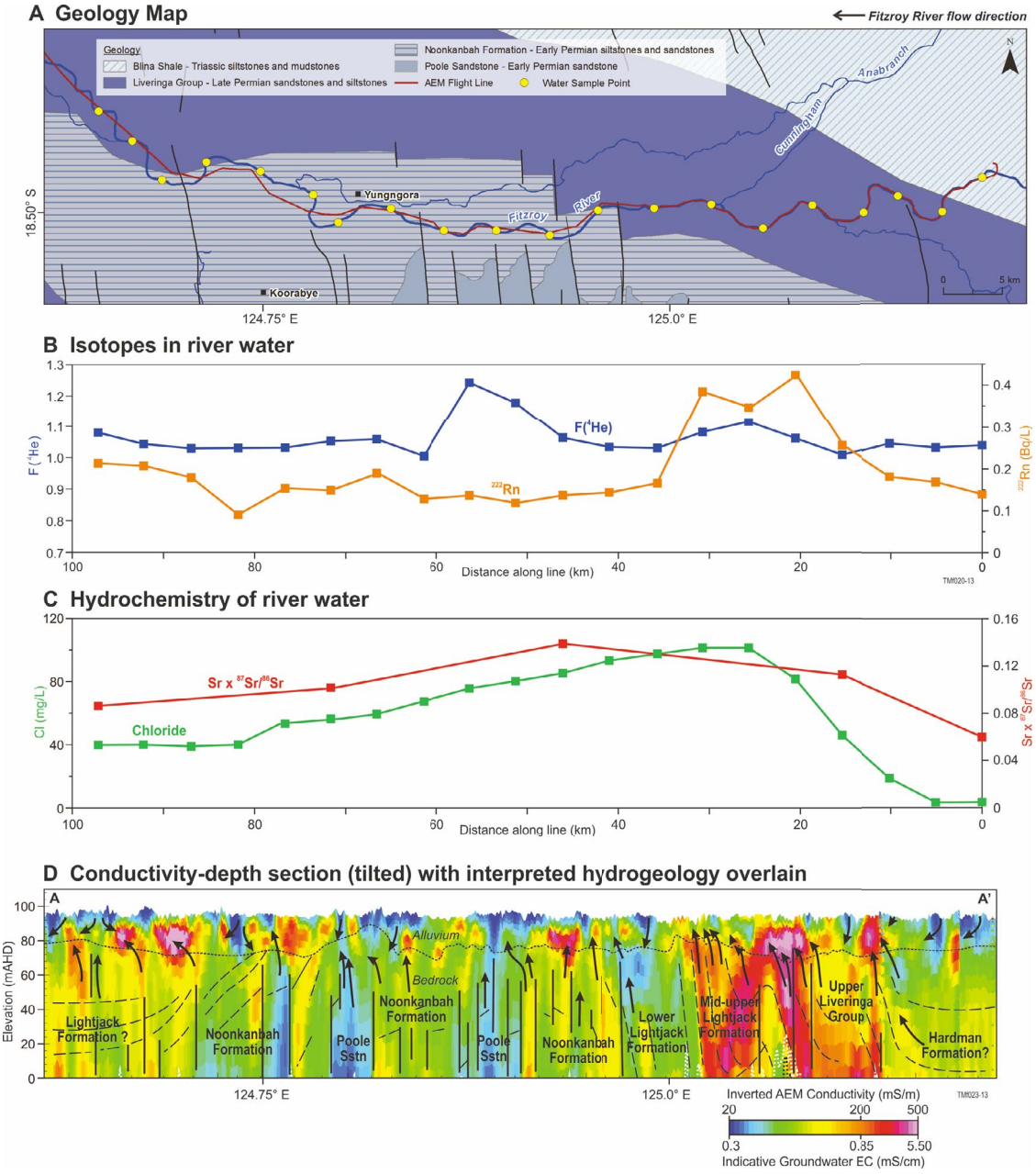

Fig. 3. Combined plot showing (A) river water sample locations and AEM survey line with respect to basement geology, (B) isotope data, (C) chemical data, and (D) an inverted conductivity-depth section with litho-stratigraphic interpretation along AEM flight path, as shown in (A). Solid black lines in (A) and (D) represent faults, dashed lines and arrows in (D) represent interpreted lithological boundaries and groundwater flow directions. The conductivity-depth section is vertically exaggerated with a V:H ratio of 1:100 (Harrington et al., 2014).

4.2. Mapping zones of groundwater–surface water exchange

A principle consequence of structural heterogeneity is that it generates variability in GW–SW connectivity. Identification of zones of enhanced GW–SW connectivity is important for informing water management and locating areas of potential environmental significance (Buss et al., 2009; Binley et al., 2013). Methods for assessing spatial variability in GW–SW exchange (e.g. seepagemeters and piezometers) can be labour intensive to install. Several geophysical applications have demonstrated how geophysics can exploit the contrasts in electrical and thermal properties of SW and GW to identify areas of GW–SW interaction at site to catchment scales more quickly. In this way geophysics can be used as a reconnaissance tool for identifying important areas for further study or as an additional data source to extrapolate information between traditional measurements.

4.2.1. Local scale mapping of groundwater–surface water interactions

Although contrasts in the electrical properties of GW and SW are relatively small in freshwater environments, several geophysical studies have been successful in revealing areas of GW–SW exchange. For instance, Mansoor et al. (2006, 2007) used waterborne ERI to detect locations of elevated pore water conductivities within an urban wetland which arose due to leaching from marginal landfill sites during rainfall events. Nyquist et al. (2008) mapped locations of GW–SW exchange within a stream section at metre-scale resolution by comparing 2D ERI sections collected at high and low stage. Differences in the inverted models were interpreted as zones of GW–SW exchange; these zones correlated with the thinning of a clay layer located beneath a carbonate aquifer and the overlying alluvium. FD-EMI methods have also been used to reveal contrasts in electrical conductivity and locate zones of GW–SW connectivity. Butler et al. (2004) used FD-EMI and seismic

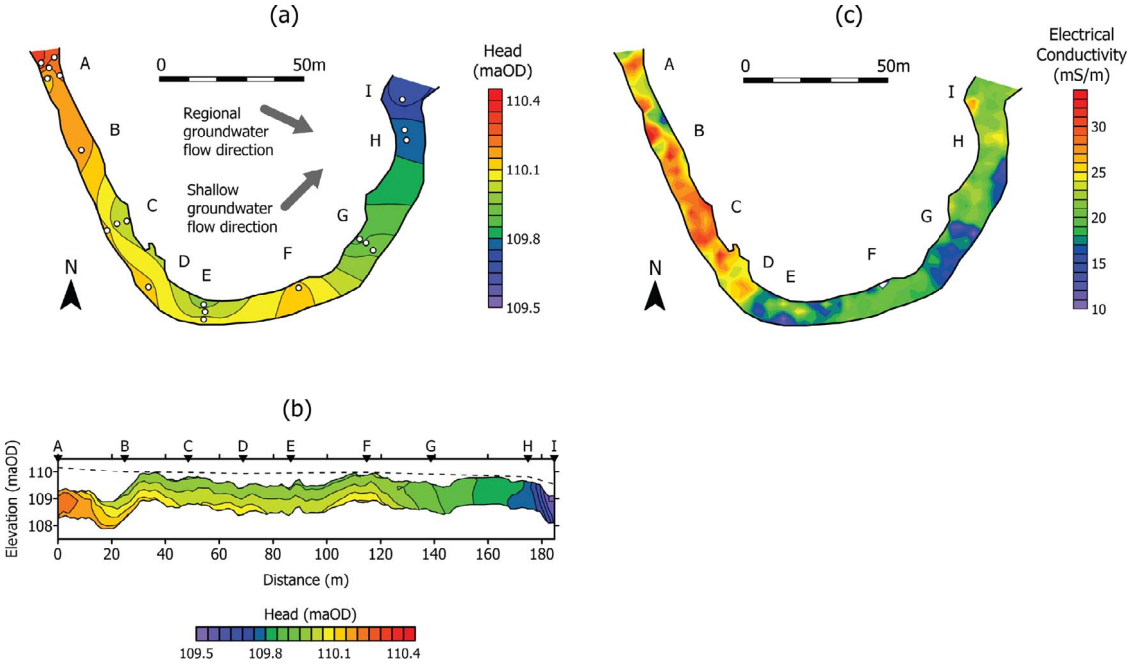

Fig. 4. Comparison of interpolated hydraulic heads obtained from piezometers and electrical conductivity obtained from waterborne FD-EMI survey. (a) Horizontal profile obtained from 100 cm deep piezometers. Symbols show measurement locations. (b) Vertical profile obtained from 20, 50, and 100 cm deep piezometers. The dashed line shows measured stage profile. (c) Map of river bed electrical conductivity obtained using Geonics EM38. Hydraulic heads are shown in metres above ordinance datum (metres above sea level) (after Binley et al., 2013).

methods to locate a clay aquitard and the extent of a clay window recharge zone. Binley et al. (2013) used waterborne FD-EMI surveys alongside piezometric data and chemical sampling (Heppell et al., 2014) to reveal spatial variability in GW discharge. Areas of high electrical conductivity were correlated with upwelling of more solute rich GW, while areas of low electrical conductivity coincided with areas exhibiting horizontal hydraulic gradients (Fig. 4).

Contrasts in electrical conductivity have also been used in coastal environments where the contrasts can be much larger. For instance, Zarroca et al. (2014) used ERI methods in association with piezometric and natural tracer data in a coastal wetland. They were able to identify zones of focused upwelling and distinguish between local and regional GW flow paths, and the intrusion of seawater which converged in the wetland. Kinnear et al. (2013) demonstrated that FD-EMI could be used to map lateral variability in electrical conductivity. They found that fresh GW discharge in the brackish Ringkøbing Fjord (Denmark) was constrained to the shoreline and demonstrated the potential for geophysical techniques to aid in assessing water budgets over larger areas.

4.2.2. Catchment scale GW–SW connectivity mapping

In a similar way as structural characterisation, there have been several applications to map GW–SW connectivity at larger scales (hundreds of metres to tens of kilometres). Paine (2003) used field based FD-EMI to determine ranges in electrical conductivity and AEM to locate salinisation sources, in addition to quantifying lateral extent and intensity of salinitisation, by developing relationships from borehole water samples in northern Texas (US). In the Venice Lagoon (Italy), Viezzoli et al. (2010) used AEM to assess saltwater intrusion in the coastal aquifer and to characterise the transition between freshwater saturated sediments and overlying saltwater saturated sediments beneath the lagoon. Kirkegaard et al. (2011) used AEM in the Ringkøbing Fjord (Denmark) finding that buried valleys beneath the lagoon were characterised by high salinity waters while some areas of the lagoon were characterised by fresher waters. ERI has also been used to map locations of GW–SW discharge. Kelly et al. (2009) used a towed waterborne ERI array and tracer data to differentiate between local and regional GW discharge along a 50 km river reach in South East Australia.

4.3. Monitoring groundwater–surface water interactions

In addition to using contrasts in the geophysical properties of GW and SW to map areas of exchange, geophysical techniques have been used to monitor and quantify processes of the GW–SW interface at local scales (metres to tens of metres). Aside from heat tracing methods, geophysical monitoring studies have almost exclusively involved ERI. However, Christiansen et al. (2011) demonstrated how time-lapse gravity measurements can be used assess river-riparian zone exchanges. ERI methods are somewhat analogous to monitoring wells in tracer experiments in that changes in resistivity are used to infer changes in hydrological properties or conditions (e.g. saturation or pore water conductivity). ERI can be used to image the entire region immediately beneath an electrode array. This means that low mobility zones, which are likely to be important in biogeochemical cycling, can be also be detected (Singha et al., 2008; Toran et al., 2013b).

Temporally distributed ERI surveys have been used at the Hanford Site (US) to monitor inland water intrusion in relation to changes in river stage and to detect high and low mobility zones in the riparian zone (Johnson et al., 2012; Wallin et al., 2013). They used time-series and time-frequency analysis to reveal the timing and location of GW–SW interactions. Cardenas and Markowski (2011) imaged a flood cycle in a dam regulated river finding that the HZ was laterally discontinuous and varied with time. In addition to surface electrodes, cross borehole ERI has been used to increase sensitivity at depths and locate areas of high and low permeability by monitoring 3D hydrological processes within the riparian zone of the Thur River, Switzerland (Coscia et al., 2011, 2012). At the Boxford riparian wetland, Uhlemann et al. (2016) found that peat exhibited a two layer behaviour separated by an intermittent clay layer; the upper layer showed a reduction in resistivity during the summer due to increased pore water conductivity and the lower layer exhibited an increase in resistivity during the winter months due to the reception of resistive GW.

Studies in fresh water environments have also used salt tracers to artificially induce electrical conductivity contrasts. For instance,

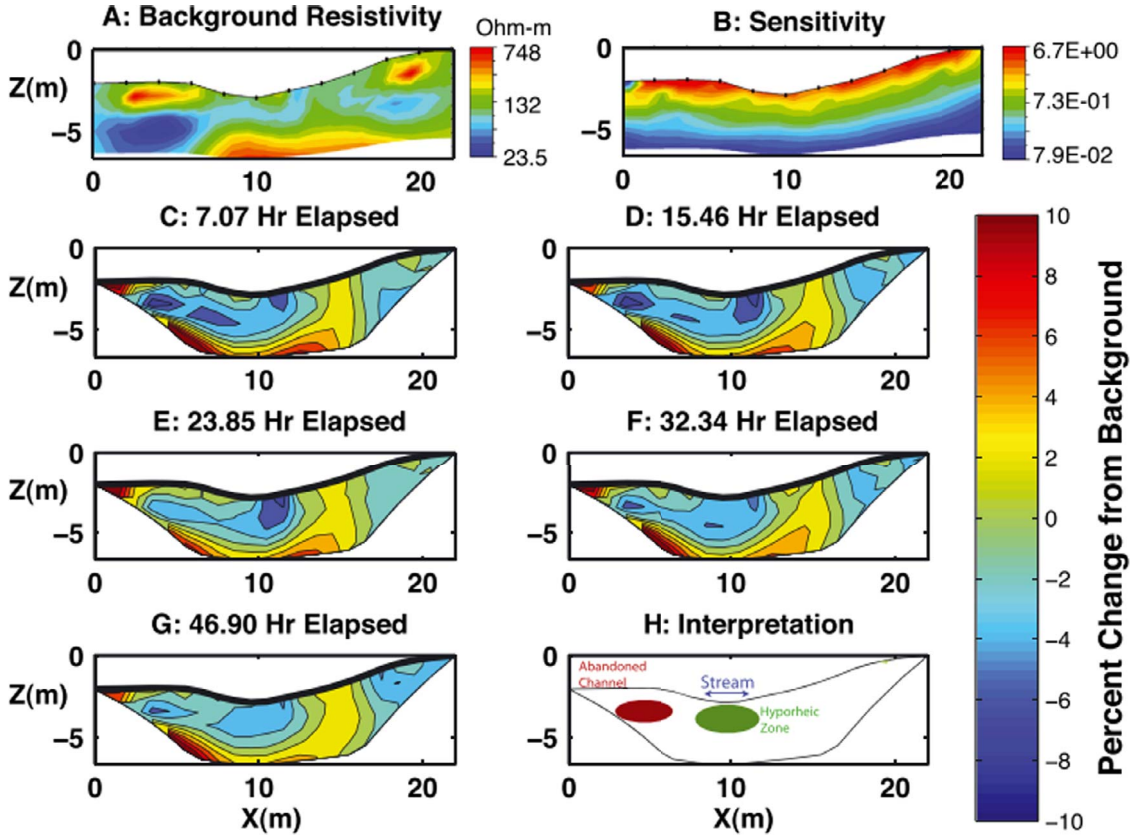

Fig. 5. Electrical resistivity imaging of solute transport in subsurface of a stream during a 21 h injection. Transects run perpendicular to the stream, with flow direction out of the page. (A) Pre-injection electrical resistivity model. (B) Model sensitivity based on the positions of electrodes in the electrode array. (C-G) Time-lapse ERI results, at time elapsed after beginning the conservative solute injection, results are shown as percentage change in resistivity from background conditions. (H) Interpretation of resistivity images. Resistive feature in pre-injection model is interpreted to be an abandoned cobble bed (Singha et al., 2015; adapted from Ward et al., 2010a).

Ward et al. (2010a) estimated the relative areas of the HZ by comparing a pre-injection ERI model with subsequent post-injection ERI models (Fig. 5). More recently, Ward et al. (2013) monitored changes in the HZ finding that hydraulic gradients parallel and perpendicular to the valley gradient had minimal influence on HZ extent and that the HZ extent increased with decreasing vertical gradients away from the stream. Similarly, Toran et al. (2013a) found that persistence of the saline tracer was more dependent on thickness and grain size rather than on the presence of restoration structures. Recently, Houzé et al. (2017) used a 3D array to obtain 7 m × 1 m × 1 m resistivity images of the subsurface following the injection of a tracer into the subsurface and note the importance of characterising boundary conditions for inverse modelling.

ERI and salt tracer studies have also been used to monitor processes in the riparian zone. To investigate the importance of voids in the riparian zone Menichino et al. (2014) created an artificial macro-pore and monitored intra-meander flow using ERI. They found that their open macro-pore enabled more solute transport and increased solute tailing, both of which are likely to be important in hydrological and biogeochemical processes. Whereas Doetsch et al. (2012b) used a 3D ERI monitoring array to estimate riparian zone infiltration velocities and found agreement with monitoring well data.

Similar to mapping zones of exchange, the natural conductivity contrasts in coastal environments can be used to monitor GW–SW interaction processes. Swarzenski et al. (2007) investigated bidirectional exchange between a coastal aquifer and sea water using ERI, electromagnetic seepage meters and geochemical tracers. They found that the tide strongly influenced hydraulic gradients such that during high tides GW discharge was reversed and sea water infiltrated into the coastal aquifer. In a similar experiment, Henderson et al. (2010) found that their ERI also indicated suppressed GW discharge, whereas temperature measurements indicated GW discharge continued at high tide. Their sensitivity modelling indicated that during high tide electrical current was preferentially focused in the conductive SW and that consequently, the resistive GW could not be easily resolved. This demonstrates the issue that methods may be limited in certain environments, it therefore highlights the importance of forward modelling to realise the sensitivity of geophysical data.

5. Discussion

Geophysical techniques have successfully provided information about processes and properties relevant to the GW–SW interface, with research focusing on three key areas: (1) characterising structure, (2) mapping zones of GW–SW interaction, and (3) monitoring dynamic processes. However, studies of properties and processes in the GW–SW interface would benefit from continued geophysical input, for which there are several avenues of potential research. In this section the strengths, challenges, and recent developments in geophysical techniques are discussed alongside opportunities for the future.

5.1. Strengths of geophysics

It is convenient to organise geophysical techniques into more general themes to consider their strengths as tools to: (1) guide more focused investigations, (2) supplement other data sets, and (3) monitor dynamic processes. These strengths are also apparent in other fields of near surface geophysics (e.g. Singha et al., 2015; Binley et al., 2015; Parsekian et al., 2015). Their presence highlights the scope of

geophysics for studies concerned with the GW–SW interface and more general environmental applications.

5.1.1. Reconnaissance tools

Often the usefulness of data can only be appreciated following the instrumentation of a site. By targeting specific sites based on preliminary geophysical investigations it may be possible to save resources and obtain more representative and useful information. In addition, at catchment scales the decision to select a particular site may be purely incidental to land access and prior instrumentation. At local scales FD-EMI (e.g. Butler et al., 2004; Binley et al., 2013) and ERI (e.g. Mansoor and Slater, 2007; Nyquist et al., 2008) have been shown to be capable of identifying zones of hydrological interest. However, geophysics has also been used to locate areas of biogeochemical interest. For example, Uhlemann et al. (2017) used ERI to guide biogeochemical and hydrological sampling of an arsenic contaminated aquifer in Cambodia (Richards et al., 2017) by characterising its sedimentological setting. In this way, geophysics can also be used to improve the confidence that intrusive data is representative or appropriate for characterisation of the site.

Additionally, geophysics has also been used as a reconnaissance tool at catchment scales; AEM has been used for locating palaeochannels (Worrall et al., 1999; Abraham et al., 2012) and areas of GW–SW connectivity (Jørgensen et al., 2012; Harrington et al., 2014). As noted by Kruse (2013), there is significant potential for combining remote sensing data with aerial and land based geophysics. These methods are highly complementary given that remote sensing data is typically sensitive to the surface and shallow subsurface (< 1 m) whereas geophysical techniques may be sensitive up to depths of several tens or hundreds of metres (Parsekian et al., 2015). Geophysics and remote sensing has been combined in permafrost studies, for instance AEM (Pastick et al., 2013) and ground based ERI and GPR (Yoshikawa and Hinzman, 2003) was used alongside remote sensing data to assess the thickness and distribution of permafrost. Approaches such as those employed by Wilson et al. (2016), whereby lakes were prioritised based on their geological setting before thermal imagery was analysed, could be enhanced by inclusion of geophysical data. The combination of remote sensing data and geophysics would be useful in linking surface and subsurface properties and would be a powerful tool in GW–SW interaction studies. Furthermore, these applications could provide additional constraints for catchment scale considerations of HEFs (e.g. Kiel and Cardenas, 2014; Gomez-Velez and Harvey, 2014).

5.1.2. Supplementing other data sets

Geophysical measurements that are sensitive to geological, hydrological or biogeochemical properties can be used to reduce interpolation uncertainty and increase the spatial coverage of information. The combination of methods has additional advantages in that by combining different data sources, poor sensitivity and other methodological limitations can be reduced. Combining data sets is common in GW–SW interface research. For instance, González-Pinzón et al. (2015) combined centimetre scale probes with chemical tracers, piezometers, fibre-optic distributed temperature sensing, temperature sensors and ERI to improve conceptual understanding of a river reach at several scales. The development of integrated and standardised approaches may also be beneficial for generating common data sets to compare field sites and improve conceptual models. Multi-method approaches are similarly used in hydrogeophysical research to combine geophysical techniques with hydrological and geophysical techniques (e.g. Moyse et al., 2005; Hinnel et al., 2010). The grouping of traditional and geophysical applications can improve the spatial extent of available information across a range of scales and improve the quantative interpretation of geophysical data. To date most geophysical studies of the GW–SW interface have focused on characterising the geological structure. Future applications should endeavour to extract information about the hydrological and biogeochemical properties of the subsurface.

5.1.3. Monitoring dynamic processes

Processes occurring at the GW–SW interface can be highly dynamic. It can be difficult to characterise these processes with traditional methods as they can interrupt processes and continuous measurements may not be possible. In this review, the ability of ERI to characterise dynamic processes has been demonstrated (e.g. Ward et al., 2010a; Johnson et al., 2012; Wallin et al., 2013). These strengths are also highlighted in related fields where ERI and IP have been used to monitor contaminant transport, biological activity and biogeochemical processes (e.g. Michot et al., 2003; Garre et al., 2011; Slater and Atekwana, 2009; Johnson et al., 2010; Flores Orozco et al., 2011; Chen et al., 2009; Singha et al., 2015). It is anticipated that knowledge from these fields could be applied to characterisation of the GW–SW interface. In addition, temporally distributed surveys of other geophysical methods may be beneficial, for example FD-EMI could be used to extend the information obtained in ERI monitoring studies and temporally distributed GPR, or seismic, surveys could be used to better characterise the dynamic nature of river bed geomorphology.

5.2. Challenges of geophysics

Despite the progress made by geophysics it is also important to appreciate the challenges of geophysical methods. These are related to geophysics in general and are on-going issues in geophysical research. The principal challenges of geophysical techniques are that: (1) geophysics is inherently uncertain, (2) site specific considerations are often needed, and (3) geophysics needs to be processed and modelled for quantitative interpretation. These limitations greatly contribute to the reluctance to adopt geophysical techniques in environmental studies. Here these challenges are discussed briefly but it is anticipated that by addressing the issues more thoroughly, application of geophysics in environmental sensing will become more common.

5.2.1. Geophysical uncertainty

Geophysical data and modelling methods are uncertain. Despite the broad recognition of errors in geophysical methods, they can be poorly dealt with and as a result, incorrect interpretations of geophysical data can be made (Binley et al., 2015). For instance, GPR and EMI survey devices often need to be corrected for instrument drift (Jacob and Hermance, 2004; De Smedt et al., 2016). Particular interest has been given to errors in ERI data. Typically, stacked or reciprocal measurements are used to assess the quality of measurements and weight them appropriately in inverse modelling (Binley, 2015; Singha et al., 2015). Stacked errors are obtained from consecutive repeat measurements for each current injection and reciprocal errors are obtained by reversing the measurement sequence and conducting a secondary survey. Reciprocal measurements are typically viewed as being more robust, as stacked measurements may underestimate measurement error (Tso et al., 2017). However, it should be noted that if the process of interest is occurring faster than a direct and reciprocal measurement scheme, then reciprocal errors may not be so useful (e.g. Ward et al., 2010a). Additionally, some studies have also looked at assessing the value of information within geophysical images in order to assess how reliable geophysical models are (e.g. Oldenburg and Li, 1999; Daily et al., 2005). For instance, Oldenburg and Li (1999) use a depth of investigation method to assess the vertical reliability of ER and IP models. More recently, JafarGardomi and Binley (2013) investigated the information content of combined ERI, FD-EMI and GPR data sets, and Nenna and Knight (2013) assessed the benefit of adding geophysical data to assess maintenance of a coastal aquifer. Methods similar to these could assist in determining the value of data assimilation and help to aid in survey design.

5.2.2. Site specific considerations

In all applications, it is important to consider the target, scale of interest and the likely subsurface properties in order to return the most

beneficial information. For instance, larger electrode spacing in ERI and IP or lower frequencies in GPR surveys will permit characterisation to deeper depths, but will sacrifice resolution (Binley et al., 2015; van der Kruk et al., 2015). Forward modelling tools such as Terry et al. (2017) can help to guide survey design based on the targets of interest and the expected subsurface properties. In some cases, geophysical surveys may also be optimised, for example in ERI electrode number, position and measurement geometry can be designed to improve spatial resolution whilst removing unnecessary measurements and consequently reducing measurement time (Wilkinson et al., 2006, 2012; Loke et al., 2015).

It is useful to briefly note some of the considerations necessary to applications in SW bodies. The water column can be problematic as it can create current focusing effects in methods influenced by electrical conductivity. For instance, in in-stream ERI surveys the depth of investigation required, the river level, and electrical conductivity of river water should be taken into consideration when deciding the electrode spacing; furthermore consideration of whether use floating arrays or bed electrodes is also important (Snyder et al., 2002). These measurements can also aid in interpretation of data (e.g. Slater et al., 2010; Binley et al., 2013). However, it should be noted that additional constraints make it more difficult to solve inverse problems and errors in measurements of water depth or in-stream electrical conductivity may generate significant inversion artefacts (Day-Lewis et al., 2006). ERI studies in SW bodies have involved static arrays (Nyquist et al., 2008; Crook et al., 2008) and towed arrays (e.g. Kelly et al., 2009; Slater et al., 2010). The latter methodology has benefits in that it can improve survey productivity; however, it precludes error quantification (Slater et al., 2010) and requires various electrode spacings to improve vertical resolution (Allen, 2007). In addition to resolution and methodology considerations, some geophysical applications may not be appropriate for the setting. For example, use of salt tracers and ERI may be prohibited in ecologically sensitive areas, or GPR signals may be attenuated in highly electrically conductive areas.

5.2.3. Extracting quantitative information

Recovering quantitative information from geophysics is a major challenge and has been the subject of numerous reviews (e.g. Rubin and Hubbard, 2005; Singha et al., 2007; 2015; Loke et al., 2013). Hydrogeological information can be extracted from geophysical data by using petrophysical relationships, interpreting time-lapse data and through combination with other techniques. Petrophysical models are commonly used due to their simplicity; however, their usage can be problematic. As noted by Singha et al. (2015) translation of geophysical images with poorly resolved heterogeneity or inversion artefacts will be erroneous, the support volumes of geophysical and hydrological parameters are often different, meaning conversions can be poor, and the resolution of geophysical images can be spatially and temporally variable such that petrophysical transformations may be inconsistent. Geophysical information can also be interpreted temporally without the need for petrophysical transformations. Johnson et al. (2012) and Wallin et al. (2013) used time-series and time-frequency analyses of the Columbia River stage and ERI to reveal preferential pathways, whereas Ward et al. (2010b) demonstrated that temporal moments of ER and solute transport data were well correlated for diffusive transport in the HZ. Geophysical data may also be interpreted from the combination with other techniques. For example, calibrating geophysical and hydrological data at point scale and estimating the correlation at field scale (Day-Lewis and Lane, 2004), by using changes in geophysical properties to calibrate hydrological models (e.g. Binley et al., 2002), or by coupled (e.g. Hinnel et al., 2010) and joint inversions (Kowalsky et al., 2005; Johnson et al., 2009).

As noted, many applications to characterise the structure of the GW–SW interface (i.e. static surveys) have been qualitative in that they are used to reveal geometry of geological deposits. Future applications should aim to characterise properties such as permeability, surface area and cation exchange capacity. Although petrophysical models are often used to translate static geophysical data following inversion, in recent years there has been increasing interest in joint inversions. Joint inversions use petrophysical relations to link multiple geophysical data sets with each other, or with hydrological data sets. They have demonstrated significant potential in recovering hydrological properties (Kowalsky et al., 2005; Johnson et al., 2009; Jardani et al., 2013; Soueid Ahmed et al., 2014, 2016) and are a promising direction for quantative interpretation of geophysical surveys of the GW–SW interface.

5.3. Recent developments in geophysical applications

Since the advent of hydrogeophysics during the 1990s (Binley, 2015), geophysical techniques have evolved from their traditional exploratory usage to being capable of characterisation of hydrological states and dynamic processes. Additionally, in more recent years the field of biogeophysics, which aims to relate the biological processes and modifications of the subsurface to geophysical properties, has emerged (Atekwana and Slater, 2009). Biogeophysical applications have typically involved characterising reactive conditions (e.g. Naudet et al., 2003; Sassen et al., 2012; Chen et al., 2013), detecting biogeochemical by-products (e.g. Slater and Binley, 2006; Comas et al., 2007; 2014; Parsekian et al., 2011), detecting changes to physical structure as a result of microbial activity (e.g. Williams et al., 2005; Slater et al., 2008), or monitoring plant-water interactions (e.g. Michot et al., 2003; Shanahan et al., 2015). In addition, the usage of unmanned vehicles in environmental research has vastly increased and it is expected that automated deployment of miniaturised geophysical devices could become common in future years. In this section developments in: (1) electrical resistivity monitoring, (2) induced polarisation, (3) self-potential, (4) multi-coil electromagnetic induction, and (5) unmanned vehicles, and their potential application in GW–SW characterisation are discussed.

5.3.1. Electrical resistivity monitoring

ERI is one of the most commonly and widely applied geophysical methods. There has been significant interest in developing low power, automated instruments for long term monitoring (e.g. Daily et al., 2004; Kuras et al., 2009; Ogilvy et al., 2009; Chambers et al., 2015). These instruments have the potential to provide spatially extensive data sets, with high spatial and temporal resolution. Moreover, instruments can also transmit data to high performance computers to allow for real time monitoring of subsurface processes (Singha et al., 2015). For instance, computational advances in inversion schemes, e.g. image differencing to avoid regularisation in the time dimension (Wallin et al., 2013) or parameterisation based on the physics of plume shape evolution (e.g. Miled and Miller, 2007; Pidlisecky et al., 2011), are promising tools for extracting hydrological information from ERI monitoring data. As noted, time-lapse ERI to monitor processes in the HZ typically do not use reciprocal measurements as a more robust estimate of error as acquisition times are perhaps too long for revealing processes of interest. ERI acquisition times could be reduced using multi-channel systems, optimised electrode arrays (e.g. Wilkinson et al., 2012), or shorter current injection. However, it should be noted that use of short injection times could result in unreliable measurements of resistivity (Binley, 2015). Also, although most studies have been conducted over periods of several hours, longer ERI monitoring studies such as that of Uhlemann et al. (2016) could be used to aid in revealing seasonal variation in GW upwelling or river-riparian zone interactions.

5.3.2. Induced polarisation

Despite being less commonly used than ERI, many modern ERI instruments are also capable of IP measurements. Although, ERI is more robust in that it has higher signal to noise ratios, the IP signal is more closely related to geological characteristics and petrophysical relationships exist for relating IP signal to surface area, permeability and cation exchange (Vinegar and Waxman, 1984; Börner and Schön, 1991; Slater et al., 2007; Revil et al., 2012; Weller and Slater, 2015). These properties

have clear relevance to the GW–SW interface, however, IP studies of the GW–SW interface have been limited (e.g. Slater et al., 2010; Mwakanyamale et al., 2012). The limited application, in comparison to ERI, is probably due to the complexity associated with analysis of data and future applications should be cautious in interpretation of IP data. Nonetheless, it is anticipated that IP would be beneficial in revealing variability in permeability, surface area and cation exchange capacity, and potentially biogeochemical processes (e.g. Flores Orozco et al., 2011; Chen et al., 2009; 2013), at the GW–SW interface.

5.3.3. Self-potential

Similar to IP, usage of SP in GW–SW interaction studies has been less frequent; however, there are several possible applications. The SP signal arises from electro-kinetic, electro-chemical, and thermo-electric sources. SP has been used to characterise hydraulic properties during pumping tests (Rizzo et al., 2004; Revil et al., 2008; Soueid Ahmed et al., 2014, 2016), through palaeochannels (Revil et al., 2005), through fractures (Wishart et al., 2006, 2008), and in arctic hill-slopes (Voytek et al., 2016). Applications in GW–SW interface research could involve assessing the spatial and temporal variability of GW discharge (e.g. Colombero et al., 2014) or HEFs, or characterising hydraulic conductivity. However, perhaps the most intriguing use of SP at the GW–SW interface would be to characterise the variability in redox conditions. SP has been used to extend the spatial coverage of redox measurements obtained from monitoring wells associated with a contaminant plume at the Entressen Landfill in France (Fig. 6) (Naudet et al., 2003, 2004; Arora et al., 2007; Linde and Revil, 2007). Naudet et al. (2004) removed the electro-kinetic contribution using piezometric head data and found that the SP signal and redox potential values showed good correlation ($R^2 = 0.85$). It is however important to note the differentiation of SP sources may be more complex in the GW–SW interface, and the electro-kinetic effect may dominate the signal. Any work involving SP would need to account for all sources of the SP signal appropriately in addition to adequate understanding of redox chemistry.

5.3.4. Multi-coil electromagnetic induction

In recent years FD-EMI instruments have been increasingly used in hydrological investigations due to their improved reliability and stability (Boaga, 2017). Furthermore, FD-EMI methods have the advantage over ERI in that they do not require contact with the ground and can therefore be more productive. Modern FD-EMI instruments contain multiple coils and are able to provide information about vertical variability in addition to lateral variability. They therefore make it possible to extend the application of FD-EMI beyond qualitative mapping of GW–SW interactions (e.g. Butler et al., 2004; Binley et al., 2013; Kinnear et al., 2013). In addition, as noted recently by Christiansen et al. (2016), the majority of studies present apparent electrical conductivity, e.g. without appropriate data processing or inverse modelling. Advances in data filtering and inversion schemes, such as EM4Soil (EMTOMO, 2013), Aarhus Workbench (Christiansen et al., 2016) or FEMIC (Elwaseif et al., 2017), permit more accurate modelling of subsurface conductivity structure and may lead to more reliable subsurface characterisation using FD-EMI

Furthermore, temporally distributed FD-EMI surveys similar to Robinson et al. (2012), Shanahan et al. (2015) and Huang et al. (2017) could prove useful in GW–SW interface characterisation. For instance, FD-EMI instruments could be used to investigate diurnal dynamics of salt water wedges in coastal environments or seasonal changes in GW upwelling, provided there are substantial contrasts in the electrical conductivity of GW and SW. It is important, however, to note that some authors (e.g. Lavoué et al., 2010) argue for the need to calibrate FD-EMI with ERI, this may be particularly true in time-lapse measurements where ambient conditions, or the operator, may influence the readings obtained.

5.3.5. Unmanned vehicles

Given the significant increase in the availability and application of automated ground-based, waterborne and aerial technology in many aspects of environmental sensing, the translation to geophysical sensing

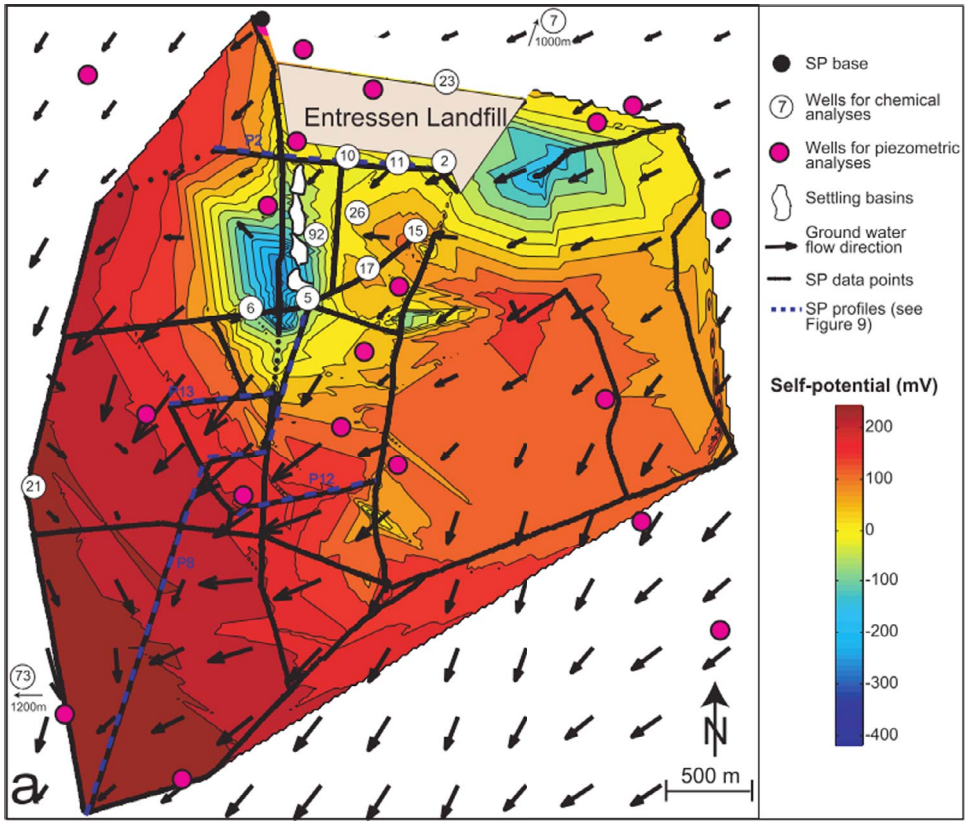

Fig. 6. Map of self-potential obtained by linear interpolation of measurements made at 10 m resolution in first 2 km from landfill site and 20 m elsewhere. Hydraulic gradients obtained from piezometers (Naudet et al., 2004).

is inevitable. Automated aerial, terrestrial and waterborne vehicles offer the ability for precise and repeatable data collection. Unmanned aerial vehicles have the ability to fly at lower elevations (~30 m) than typical aircraft, and are therefore able to provide high resolution data sets without sacrificing productivity. Geophysical applications using automated vehicles have predominantly involved magnetic mapping to locate manmade features (Stoll, 2013; Phelps et al., 2014). Automated vehicles may also be able to simultaneously process and contour data, and transmit information in real time (Phelps et al., 2014). Furthermore, automated systems could be programmed in such a way that anomalous regions are re-surveyed in higher resolution automatically.

The majority of unmanned aerial vehicles are small (< 25 kg) and are limited to light weight instruments, however larger vehicles capable of carrying heavier payloads are available (Whitehead et al., 2014a, 2014b). It can be envisaged that miniaturisation (or weight reduction) of geophysical tools, and the increasing pay loads of UAVs, could allow for increased collection of automated aerial geophysical data. However, non-aerial geophysical applications could easily be adapted to use automated vehicles, for instance roving surveys using plate electrodes for ERI (Christensen and Sørensen, 1998), large scale FD-EMI surveys (Christiansen et al., 2016) or waterborne surveys (Kelly et al., 2009; Binley et al., 2013; Colombero et al., 2014) would not be difficult to automate and may aid in collection of data across larger scale, e.g. to investigate parameters at catchment scales.

6. Summary

Geophysical tools have clear application in revealing geological, hydrological and biogeochemical heterogeneity at the GW–SW interface. Geophysical tools are highly complementary to traditional tools as they are sensitive to regions of the subsurface not always reachable by direct measurements. The majority of geophysical applications have focused on characterising subsurface structure, revealing spatial variability in GW–SW interaction and imaging hydrological processes. Data sets obtained from these field studies have significant potential to improve characterisation and modelling of parameters at the GW–SW interface. Over the last 20 years geophysical methods have grown to be powerful tools in hydrogeological research, in part due to the view that geophysical tools be used to aid hydrogeological problems alongside traditional methods. Geophysics provides valuable practical tools for assessing many unknowns of the GW–SW interface. Moreover, although caution in quantative interpretation of geophysical data is warranted, attempts at improving uncertainty quantification, inversion routines and translating data are on-going. Efforts to provide solutions to these issues can only continue to improve confidence in geophysics so that its potential can be more widely appreciated and applied across a variety of scales. In recent years, there has been significant development in techniques and methodologies in parallel research areas, some of which would enhance the information obtained in studies of the GW–SW interface. Continued integration of geophysical methods would be beneficial in characterising hydrological and biogeochemical heterogeneity in the GW–SW interface and understanding the implications for water quality and ecological health.

Acknowledgements

We are grateful to André Revil, Kamini Singha and an anonymous reviewer for their comments on an earlier version of the manuscript. This work is supported by the NERC Envision Doctoral Training Programme (GA/15S/004 S301). The contributions of J. Chambers and S. Uhlemann are published with the permission of the Executive Director of the British Geological Survey (NERC).

References

Abraham, J.D., Cannia, J.C., Bedrosian, P.A., Johnson, M.R., Ball, L.B., Sibray, S.S., 2012. Airborne Electromagnetic Mapping of the Base of Aquifer in Areas of Western Nebraska. pp. 1–38. US Geological Survey Scientific Investigations Report 2011-5219. https://pubs.usgs.gov/sir/2011/5219/.

Allen, D.A., 2007. Electrical Conductivity Imaging of Aquifers Connected to Watercourse. Faculty of Science, University of Technology, Sydney, pp. 1–438.

Anderson, N.L., Ismael, A.M., Thitimakorn, T., 2007. Ground-penetrating radar: a tool for monitoring bridge scour. Environ. Eng. Geosci. 13 (1), 1–10. http://pubs.er.usgs.gov/publication/70031991.

Annan, A.P., 2005. GPR methods for hydrogeological studies. In: Rubin, Y., Hubbard, S.S. (Eds.), Hydrogeophysics. Springer, Netherlands, pp. 185–213.

Archie, G.E., 1942. The electrical resistivity log as an aid in determining some reservoir characteristics. Trans. Am. Inst. Min. Metall. Eng. 146, 54–62. https://doi.org/10.2118/942054-G.

Arora, T., Linde, N., Revil, A., Castermant, J., 2007. Non-intrusive characterization of the redox potential of landfill leachate plumes from self-potential data. J. Contam. Hydrol. 92, 274–292. https://doi.org/10.1016/j.jconhyd.2007.01.018.

Aster, R., Borchers, B., Thurbur, C., 2005. Parameter Estimation and Inverse Problems, 2nd ed. Academic Press, New York, US.

Atekwana, E.A., Slater, L.D., 2009. Biogeophysics: a new frontier in Earth science research. Rev. Geophys. 47, 1–30. https://doi.org/10.1029/2009RG000285.

Ball, L.B., Kress, W.H., Cannia, J.C., 2006. Determination of Canal Leakage Potential Using Continuous Resistivity Profiling Techniques in Western Nebraska and Eastern Wyoming, 2004. pp. 1–53 US Geological Survey Scientific Investigations Report 2006-5032. https://pubs.water.usgs.gov/sir20065032.

Bencala, K.E., 1984. Interactions of solutes and streambed sediment: 2. A dynamic analysis of coupled hydrologic and chemical processes that determine solute transport. Water Resour. Res. 20 (12), 1804–1814. https://doi.org/10.1029/WR020i012p01804.

Bencala, K.E., Kennedy, K.C., Zellweger, G.W., Jackman, A.P., Avanzino, R.J., 1984. Interactions of solutes and streambed sediment: 1. An experimental analysis of cation and anion transport in a mountain stream. Water Resour. Res. 20 (12), 1797–1803. http://onlinelibrary.wiley.com/doi/10.1029/WR020i012p01797/full.

Bianchin, M.S., Smith, L., Beckie, R.D., 2011. Defining the hyporheic zone in a large tidally influenced river. J. Hydrol. 406, 16–29. https://doi.org/10.1016/j.jhydrol.2011.05.056.

Binley, A., Cassiani, G., Middleton, R., Winship, P., 2002. Vadose zone flow model parameterisation using cross-borehole radar and resistivity imaging. J. Hydrol. 267 (3–4), 147–159. https://doi.org/10.1016/S0022-1694(02)00146-4.

Binley, A., Slater, L.D., Fukes, M., Cassiani, G., 2005. Relationship between spectral induced polarization and hydraulic properties of saturated and unsaturated sandstone. Water Resour. Res. 41 (W12417), 1–13. https://doi.org/10.1029/2005WR004202.

Binley, A., Ullah, S., Heathwaite, L., Heppell, C., Byrne, P., Lansdown, K., Trimmer, M., Zhang, H., 2013. Revealing the spatial variability of water fluxes at the groundwater–surface water interface. Water Resour. Res. 49 (7), 3978–3992. https://doi.org/10.1002/wrcr.20214.

Binley, A., 2015. Tools and techniques: electrical methods. In: Schubert, G. (Ed.), 2nd ed. Treatise on Geophysics 11. Elsevier, Oxford, UK, pp. 233–259. https://doi.org/10.1016/B978-0-444-53802-4.00192-5.

Binley, A., Hubbard, S.S., Huisman, J.A., Revil, A., Robinson, D.A., Singha, K., Slater, L.D., 2015. The emergence of hydrogeophysics for improved understanding of subsurface processes over multiple scales. Water Resour. Res. 51 (6), 3837–38366. https://doi.org/10.1002/2015WR017016.

Boaga, J., 2017. The use of FDEM in hydrogeophysics: a review. J. Appl. Geophys. 139, 36–46. https://doi.org/10.1016/j.jappgeo.2017.02.011.

Boano, F., Revelli, R., Ridolfi, L., 2008. Reduction of the hyporheic zone volume due to the stream-aquifer interaction. Geophys. Res. Lett. 35 (9), 1–5. L09401. https://doi.org/10.1029/2008GL033554.

Boano, F., Poggi, D., Revelli, R., Ridolfi, L., 2009. Gravity-driven water exchange between streams and hyporheic zones. Geophys. Res. Lett. 36 (20), 1–5. https://doi.org/10.1029/2009GL040147.

Boano, F., Harvey, J.W., Marion, A., Packman, A.I., Revelli, R., Ridolfi, L., Wörman, A., 2014. Hyporheic flow and transport processes: mechanisms, models, and biogeochemical implications. Rev. Geophys. 52 (4), 603–679. https://doi.org/10.1002/2012RG000417.

Börner, F.D., Schön, J.H., 1991. Technical Note: A Relation Between the Quadrature Component of Electrical Conductivity and the Specific Surface Area of Sedimentary Rocks 32. Society of Petrophysicists and Well-Log Analysts, pp. 612–613.

Boulton, A.J., Findlay, S., Marmonier, P., Stanley, E.H., Valett, H.M., 1998. The functional significance of the hyporheic zone in streams and rivers. Annu. Rev. Ecol. Syst. 29, 59–81. https://doi.org/10.1146/annurev.ecolsys.29.1.59.

Boulton, A.J., Datry, T., Kasahara, T., Mutz, M., Stanford, J.A., 2010. Ecology and management of the hyporheic zone: stream–groundwater interactions of running waters and their floodplains. J. N. Am. Benthol. Soc. 29 (1), 26–40. https://doi.org/10.1899/08-017.1.

Bridge, J.W., 2005. High Resolution In-Situ Monitoring of Hyporheic Zone Biogeochemistry. pp. 1–44 UK Environment Agency Science Report SC030155/SR3.

Brunet, P., Clément, R., Bouvier, C., 2010. Monitoring soil water content and deficit using Electrical Resistivity Tomography (ERT) – a case study in the Cevennes area, France. J. Hydrol. 380 (1–2), 146–153. https://doi.org/10.1016/j.jhydrol.2009.10.032.

Brunke, M., Gonser, T., 1997. The ecological significance of exchange processes between rivers and groundwater. Freshw. Biol. 37 (1), 1–33. https://doi.org/10.1046/j.1365-2427.1997.00143.x.

Buss, S.R., Cai, Z., Cardenas, B., Fleckenstein, J., Hannah, D.M., Hepell, K., Hulme, P., Ibrahim, T., Käser, D., Krause, S., Lawler, D.., Lerner, D., Mant, J., Malcolm, I., Old, G., Parkin, G., Pickup, R., Pinay, G., Porter, J., Rhoes, G., Richie, A., Riley, J., Robertson, A., Sear, D., Shields, B., Smith, J., Tellam, J., Wood, P., 2009. The

Hyporheic Handbook: A Handbook on the Groundwater–Surface Water Interface and Hyporheic Zone for Environment Managers Integrated Catchment Science Programme. pp. 1–264 UK Environment Agency Science Report SC050070.
Butler, K.E., Nadeau, J., Parrott, R., Daigle, A., 2004. Delineating recharge to a river valley aquifer by riverine seismic and EM methods. J. Environ. Eng. Geophys. 9 (2), 95–109. http://library.seg.org/doi/abs/10.4133/JEEG9.2.95.
Cardenas, M.B., Markowski, M.S., 2011. Geoelectrical imaging of hyporheic exchange and mixing of river water and groundwater in a large regulated river. Environ. Sci. Technol. 45 (4), 1407–1411. https://doi.org/10.1021/es103438a.
Chambers, J.E., Gunn, D.A., Wilkinson, P.B., Meldrum, P.I., Haslam, E., Holyoake, S., Kirkham, M., Kuras, O., Merrit, A., Wragg, J., 2014a. 4D electrical resistivity tomography monitoring of soil moisture dynamics in an operational railway embankment. Near Surf. Geophys. 12 (1), 61–72. https://doi.org/10.3997/1873-0604.2013002.
Chambers, J.E., Wilkinson, P.B., Uhlemann, S., Sorensen, J.P.R., Roberts, C., Newell, A.J., Ward, W.O.C., Binley, A., Williams, P.J., Goody, D.C., Old, G., Bai, L., 2014b. Derivation of lowland riparian wetland deposit architecture using geophysical image analysis and interface detection. Water Resour. Res. 50 (7), 5886–5905. https://doi.org/10.1002/2012WR013085.
Chambers, J.E., Meldrum, P.I., Wilkinson, P.B., Ward, W., Jackson, C., Matthews, B., Joel, P., Kuras, O., Bai, L., Uhlemann, S., Gunn, D., 2015. Spatial monitoring of groundwater drawdown and rebound associated with quarry dewatering using automated time-lapse electrical resistivity tomography and distribution guided clustering. Eng. Geol. 193, 412–420. https://doi.org/10.1016/j.enggeo.2015.05.015.
Chandler, I.D., Guymer, I., Pearson, J.M., van Egmond, R., 2016. Vertical variation of mixing within porous sediment beds below turbulent flows I. Water Resour. Res. 52, 3493–3509. https://doi.org/10.1002/2015WR018274.
Chen, J., Hubbard, S.S., Williams, K.H., Pride, S., Li, L., Steefel, C., Slater, L., 2009. A state-space Bayesian framework for estimating biogeochemical transformations using time-lapse geophysical data. Water Resour. Res. 45 (8). W08420, 1–15. https://doi.org/10.1029/2008WR007698.
Chen, J., Hubbard, S.S., Williams, K.H., 2013. Data-driven approach to identify field-scale biogeochemical transitions using geochemical and geophysical data and hidden Markov models: development and application at a uranium-contaminated aquifer. Water Resour. Res. 49 (10), 6412–6424. https://doi.org/10.1002/wrcr.20524.
Christensen, N.B., Sørensen, K.I., 1998. Surface and borehole electric and electromagnetic methods for hydrogeological investigations. Eur. J. Eng. Environ. Geophys. 3 (1), 75–90.
Christiansen, A., Pedersen, J., Auken, E., Søe, N., Holst, M., Kristiansen, S., 2016. Improved geoarchaeological mapping with electromagnetic induction instruments from dedicated processing and inversion. Remote Sens. 8 (12), 1022. https://doi.org/10.3390/rs8121022.
Christiansen, L., Binning, P.J., Rosbjerg, D., Andersen, O.B., Bauer-Gottwein, P., 2011. Using time-lapse gravity for groundwater model calibration: an application to alluvial aquifer storage. Water Resour. Res. 47 (6), 1–12. W06503. https://doi.org/10.1029/2010WR009859.
Colombero, C., Comina, C., Gianotti, F., Sambuelli, L., 2014. Waterborne and on-land electrical surveys to suggest the geological evolution of a glacial lake in NW Italy. J. Appl. Geophys. 105, 191–202. https://doi.org/10.1016/j.jappgeo.2014.03.020.
Comas, X., Slater, L., Reeve, A., 2007. In situ monitoring of free-phase gas accumulation and release in peatlands using ground penetrating radar (GPR). Geophys. Res. Lett. 34 (6), 1–5. L06402. https://doi.org/10.1029/2006GL029014.
Comas, X., Kettridge, N., Binley, A., Slater, L., Parsekian, A., Baird, A.J., Strack, M., Waddington, J.M., 2014. The effect of peat structure on the spatial distribution of biogenic gases within bogs. Hydrol. Process. 28 (22), 5483–5494. https://doi.org/10.1002/hyp.10056.
Constable, S.C., 1987. Occam's inversion: A practical algorithm for generating smooth models from electromagnetic sounding data. Geophysics 52 (3), 289–300. https://doi.org/10.1190/1.1442303.
Cook, P.G., Herczeg, A.L., 2000. Environmental Tracers in Subsurface Hydrology. Springer, New York, US. https://link.springer.com/book/10.1007%2F978-1-4615-4557-6.
Coscia, I., Greenhalgh, S.A., Linde, N., Doetsch, J., Marescot, L., Günther, T., Vogt, T., Green, A.G., 2011. 3D crosshole ERT for aquifer characterization and monitoring of infiltrating river water. Geophysics 76 (2), G49–G59. https://doi.org/10.1190/1.3553003.
Coscia, I., Linde, N., Greenhalgh, S., Vogt, T., Green, A., 2012. Estimating traveltimes and groundwater flow patterns using 3D time-lapse crosshole ERT imaging of electrical resistivity fluctuations induced by infiltrating river water. Geophysics 77 (4), E239–E250. https://doi.org/10.1190/geo2011-0328.1.
Crook, N., Zarnetske, J., Haggerty, R., Robinson, D.A., Binley, A., Knight, R., Zarnetske, J., Haggerty, R., 2008. Electrical resistivity imaging of the architecture of substream sediments. Water Resour. Res. 44 (4), 1–11. W00D13. https://doi.org/10.1029/2008WR006968.
Daily, W., Ramirez, A., Binley, A., 2004. Remote monitoring of leaks in storage tanks using electrical resistance tomography: application at the Hanford site. J. Environ. Eng. Geophys. 9 (1), 11–24. http://dx.doi.org/10.4133/JEEG9.1.11.
Daily, W., Ramirez, A., Binley, A., LaBrecque, D., 2005. Electrical resistance tomography-theory and practice. In: Butler, D.K. (Ed.), Near-Surface Geophysics. Society of Exploration Geophysicists, Oklahoma, US, pp. 525–550. http://dx.doi.org/10.1190/1.9781560801719.
Day-Lewis, F.D., Lane, J.W., 2004. Assessing the resolution-dependent utility of tomograms for geostatistics. Geophys. Res. Lett. 31 (7), 1–4. L07503. https://doi.org/10.1029/2004GL019617.
Day-Lewis, F.D., White, E.A., Johnson, C.D., Lane, J.W., Belaval, M., 2006. Continuous resistivity profiling to delineate submarine groundwater discharge—examples and limitations. Lead. Edge 25 (6), 724–728. http://library.seg.org/doi/abs/10.1190/1.2210056.
De Smedt, P., Delefortrie, S., Wyffels, F., 2016. Identifying and removing micro-drift in ground-based electromagnetic induction data. J. Appl. Geophys. 131, 14–22. https://doi.org/10.1016/j.jappgeo.2016.05.004.
Doetsch, J., Linde, N., Pessognelli, M., Green, A.G., Günther, T., 2012a. Constraining 3-D electrical resistance tomography with GPR reflection data for improved aquifer characterization. J. Appl. Geophys. 78, 68–76. https://doi.org/10.1016/j.jappgeo.2011.04.008.
Doetsch, J., Linde, N., Vogt, T., Binley, A., Green, A.G., 2012b. Imaging and quantifying salt-tracer transport in a riparian groundwater system by means of 3D ERT monitoring. Geophysics 77 (5), B207–B218. https://doi.org/10.1190/geo2012-0046.1.
Dorn, C., Linde, N., Borgne, T.Le, Bour, O., Baron, L., 2011. Single-hole GPR reflection imaging of solute transport in a granitic aquifer. Geophys. Res. Lett. 1–11. https://doi.org/10.1029/2011GL047152.1.
Doro, K.O., Leven, C., Cirpka, O.A., 2013. Delineating subsurface heterogeneity at a loop of River Steinlach using geophysical and hydrogeological methods. Environ. Earth Sci. 69, 335–348. https://doi.org/10.1007/s12665-013-2316-0.
Dudley-Southern, M., Binley, A., 2015. Temporal responses of groundwater–surface water exchange to successive storm events. Water Resour. Res. 51 (2), 1112–1126. https://doi.org/10.1002/2014WR016259.
Elliott, H., Brooks, N.H., 1997. Transfer of nonsorbing solutes to a streambed with bed forms: theory. Water Resour. Res. 33 (1), 123–136.
Elwaseif, M., Robinson, J., Day-Lewis, F.D., Ntarlagiannis, D., Slater, L.D., Lane Jr., J.W., Minsley, B.J., Schultz, G., 2017. A matlab-based frequency-domain electromagnetic inversion code (FEMIC) with graphical user interface. Comput. Geosci. 99, 61–71. https://doi.org/10.1016/j.cageo.2016.08.016.
EMTOMO, 2013. EM4Soil: Software for Electromagnetic Tomography. http://www.emtomo.com/.
Everett, M.E., Meju, M.A., 2005. Electromagnetic induction. In: Rubin, Y., Hubbard, S.S. (Eds.), Hydrogeophysics 2. Springer, Netherlands, pp. 157–183. https://doi.org/10.1080/00107516108202659.
Findlay, S., Strayer, D., Goumbala, C., Gould, K., 1993. Metabolism of streamwater dissolved organic carbon in the shallow hyporheic zone. Limnol. Oceanogr. 38 (7), 1493–1499. https://doi.org/10.4319/lo.1993.38.7.1493.
Findlay, S., 1995. Importance of surface-subsurface exchange in stream ecosystems: the hyporheic zone. Limnol. Oceanogr. 40 (1), 159–164. https://doi.org/10.4319/lo.1995.40.1.0159.
Fitterman, D.V., 2015. Tools and techniques: active-source electromagnetic methods. In: Schubert, G. (Ed.), 2nd ed. Treatise on Geophysics 11. Elsevier, Oxford, UK, pp. 233–259. https://doi.org/10.1016/B978-0-444-53802-4.00193-7.
Fleckenstein, J.H., Krause, S., Hannah, D.M., Boano, F., 2010. Groundwater-surface water interactions: new methods and models to improve understanding of processes and dynamics. Adv. Water Res. 33 (11), 1291–1295. https://doi.org/10.1016/j.advwatres.2010.09.011.
Flores Orozco, A., Williams, K.H., Long, P.E., Hubbard, S.S., Kemna, A., 2011. Using complex resistivity imaging to infer biogeochemical processes associated with bioremediation of an uranium-contaminated aquifer. J. Geophys. Res.: Biogeosci. 116 (3), 1–17. https://doi.org/10.1029/2010JG001591.
Freeze, R.A., Witherspoon, P.A., 1967. Theoretical analysis regional groundwater flow: 2. Effect of water-table configuration and subsurface permeability variation. Water Resour. Res. 3 (2), 623–634. http://onlinelibrary.wiley.com/doi/10.1029/WR003i002p00623.
Froese, D.G., Smith, D.G., Clement, D.T., 2005. Characterizing large river history with shallow geophysics: Middle Yukon River, Yukon Territory and Alaska. Geomorphology 67 (3–4), 391–406. https://doi.org/10.1016/j.geomorph.2004.11.011.
Gallardo, L.A., Meju, M.A., 2004. Joint two-dimensional DC resistivity and seismic travel time inversion with cross-gradients constraints. J. Geophys. Res. 109, 1–11. https://doi.org/10.1029/2003JB002716.
Gandy, C.J., Smith, J.W.N., Jarvis, A.P., 2007. Attenuation of mining-derived pollutants in the hyporheic zone: a review. Sci. Total Environ. 373 (2–3), 435–446. https://doi.org/10.1016/j.scitotenv.2006.11.004.
Garré, S., Javaux, M., Vanderborght, J., Pagès, L., Vereecken, H., 2011. Three-dimensional electrical resistivity tomography to monitor root zone water dynamics. Vadose Zone J. 10 (1), 412–424.
Glover, P.W.J., 2015. Geophysical properties of the near surface earth: electrical properties. In: Schubert, G. (Ed.), 2nd ed. Treatise on Geophysics 11. Elsevier, Oxford, UK, pp. 89–137. https://doi.org/10.1016/B978-0-444-53802-4.00190-1.
Gomez-Velez, J.D., Harvey, J.W., 2014. A hydrogeomorphic river network model predicts where and why hyporheic exchange is important in large basins. Geophys. Res. Lett. 41 (18), 6403–6412. https://doi.org/10.1002/2014GL061099.
González-Pinzón, R., Ward, A.S., Hatch, C.E., Wlostowski, A.N., Singha, K., Gooseff, M.N., Haggerty, R., Harvey, J.W., Cirpka, O.A., Brock, J.T., 2015. A field comparison of multiple techniques to quantify groundwater–surface-water interactions. Freshw. Sci. 34 (1), 139–160. https://doi.org/10.1086/679738.
Gooseff, M.N., 2010. Defining hyporheic zones– advancing our conceptual and operational definitions of where stream water and groundwater meet. Geogr. Compass 4 (8), 945–955.
Greswell, R.B., 2005. High-resolution In Situ Monitoring of Flow Between Aquifers and Surface Waters. pp. 1–44 UK Environment Agency Science Report SC030155/SR4.
Günther, T., Rucker, C., 2006. A new joint inversion approach applied to the combined tomography of DC resistivity and refraction data. In: Proceedings of the 19th EEGS Annual Meeting. Seattle, USA.
Hare, D.K., Briggs, M.A., Rosenberry, D.O., Boutt, D.F., Lane, J.W., 2015. A comparison of thermal infrared to fiber-optic distributed temperature sensing for evaluation of groundwater discharge to surface water. J. Hydrol. 530, 153–166. https://doi.org/

10.1016/j.jhydrol.2015.09.059.
Harrington, G.A., Payton Gardner, W., Munday, T.J., 2014. Tracking groundwater discharge to a large river using tracers and geophysics. Ground Water 52 (6), 837–852. https://doi.org/10.1111/gwat.12124.
Harvey, J.W., Germann, P.F., Odum, W.E., 1987. Geomorphological control of subsurface hydrology in the creekbank zone of tidal marshes. Estuar. Coast. Shelf Sci. 25, 677–691.
Harvey, J.W., Wagner, B.J., Bencala, K.E., 1996. Evaluating the reliability of stream tracer approach to characterize stream-subsurface water exchange. Water Resour. Res. 32 (8), 2441–2451. http://onlinelibrary.wiley.com/doi/10.1029/96WR01268.
Harvey, J.W., Fuller, C.C., 1998. Effect of enhanced manganese oxidation in the hyporheic zone on basin-scale geochemical mass balance. Water Resour. Res. 34 (4), 623–636. https://doi.org/10.1029/97WR03606.
Harvey, J.W., Drummond, J.D., Martin, R.L., McPhillips, L.E., Packman, A.I., Jerolmack, D.J., Stonedahl, S.H., Aubeneau, A.F., Sawyer, A.H., Larsen, L.H., Tobias, C.R., 2012. Hydrogeomorphology of the hyporheic zone : Stream solute and fine particle interactions with a dynamic streambed. J. Geophys. Res. 117 (G00N11), 1–20. https://doi.org/10.1029/2012JG002043.
Harvey, J.W., Gooseff, M.N., 2015. River corridor science: Hydrologic exchange and ecological consequences from bedforms to basins. Water Resour. Res. 51 (9), 6893–6922. https://doi.org/10.1002/2015WR017617.
Hayashi, M., Rosenberry, D.O., 2002. Effects of ground water exchange on the hydrology and ecology of surface water. Ground Water 40 (3), 309–316.
He, X., Koch, J., Sonnenborg, T.O., Jorgensen, F., Schamper, C., Refsgaard, J.C., 2014. Transition probability-based stochastic geological modeling using airborne geophysical data and borehole data. Water Resour. Res. 50 (4), 3147–3169. https://doi.org/10.1002/2013WR014593.
Henderson, R.D., Day-Lewis, F.D., Abarca, E., Harvey, C.F., Karam, H.N., Liu, L., Lane, J.W.J., 2010. Marine electrical resistivity imaging of submarine groundwater discharge: sensitivity analysis and application in Waquoit Bay, Massachusetts, USA. Hydrogeol. J. 18, 173–185. https://doi.org/10.1007/s10040-009-0498-z.
Heppell, C., Louise Heathwaite, A., Binley, A., Byrne, P., Ullah, S., Lansdown, K., Keenan, P., Trimmer, M., Zhang, H., 2014. Interpreting spatial patterns in redox and coupled water–nitrogen fluxes in the streambed of a gaining river reach. Biogeochemistry 117 (2), 491–509. https://doi.org/10.1007/s10533-013-9895-4.
Herckenrath, D., Fiandaca, G., Auken, E., Bauer-Gottwein, P., 2013. Sequential and joint hydrogeophysical inversion using a field-scale groundwater model with ERT and TDEM data. Hydrol. Earth Syst. Sci. 17 (10), 4043–4060. https://doi.org/10.5194/hess-17-4043-2013.
Hering, D., Borja, A., Carstensen, J., Carvalho, L., Elliott, M., Feld, C.K., Heiskanen, A.S., Johnson, R.K., Moe, J., Pont, D., Solheim, A.L., van de Bund, W., 2010. The European water framework directive at the age of 10: a critical review of the achievements with recommendations for the future. Sci. Total Environ. 408 (19), 4007–4019. https://doi.org/10.1016/j.scitotenv.2010.05.031.
Hester, E.T., Cardenas, M.B., Haggerty, R., Apte, S.V., 2017. The importance and challenge of hyporheic mixing. Water Resour. Res. 53, 3565–3575. https://doi.org/10.1002/2016WR020005.
Hester, E.T., Young, K.I., Widdowson, M.A., 2013. Mixing of surface and groundwater induced by riverbed dunes: Implications for hyporheic zone definitions and pollutant reactions. Water Resour. Res. 49 (9), 5221–5237. https://doi.org/10.1002/wrcr.20399.
Hinnell, A.C., Ferré, T.P.A., Vrugt, J.A., Huisman, J.A., Moysey, S., Rings, J., Kowalsky, M.B., 2010. Improved extraction of hydrologic information from geophysical data through coupled hydrogeophysical inversion. Water Resour. Res. 46 (4), 1–14. W00D40. https://doi.org/10.1029/2008WR007060.
Holliger, K., 2008. Groundwater geophysics: from structure and porosity towards permeability? In: Darnault, C.J.G. (Ed.), Overexploitation and Contamination of Shared Groundwater Resources: Management, (Bio)Technological, and Political Approaches to Avoid Conflicts. Springer, Dordrecht, Netherlands. https://doi.org/10.1007/978-1-4020-6985-7_4.
Hoversten, G.M., Cassassuce, F., Gasperikova, E., Newman, G.A., Chen, J., Rubin, Y., Hou, Z., Vasco, D., 2006. Direct reservoir parameter estimation using joint inversion of marine seismic AVA and CSEM data. Geophysics 71 (3), C1–C13.
Huang, J., Scudiero, E., Clary, W., Corwin, D.L., Triantafilis, J., 2017. Time-lapse monitoring of soil water content using electromagnetic conductivity imaging. Soil Use Manag. 33, 191–204. https://doi.org/10.1111/sum.12261.
Hubbard, S.S., Linde, N., 2011. Hydrogeophysics. In: Wilderer, P. (Ed.), Treatise on Water Science 2. Academic Press, Oxford, UK, pp. 401–432.
Huisman, J.A., Hubbard, S.S., Redman, J.D., Annan, A.P., 2003. Measuring soil water content with ground penetrating radar: a review. Vadose Zone J. 2, 476–491.
Huisman, J.A., Rings, J., Vrugt, J.A., Sorg, J., Vereecken, H., 2010. Hydraulic properties of a model dike from coupled Bayesian and multi-criteria hydrogeophysical inversion. J. Hydrol. 380 (1–2), 62–73. https://doi.org/10.1016/j.jhydrol.2009.10.023.
Ingham, M., McConchie, J.A., Wilson, S.R., Cozens, N., 2006. Measuring and monitoring saltwater intrusion in shallow unconfined coastal aquifers using direct current resistivity traverses. J. Hydrol. N. Z. 45 (2), 69–82.
Irvine, D.J., Lautz, L.K., 2015. High resolution mapping of hyporheic fluxes using streambed temperatures: recommendations and limitations. J. Hydrol. 524, 137–146. https://doi.org/10.1016/j.jhydrol.2015.02.030.
Irvine, D.J., Cartwright, I., Post, V.E.A., Simmons, C.T., Banks, E.W., 2016. Uncertainties in vertical groundwater fluxes from 1-D steady state heat transport analyses caused by heterogeneity, multidimensional flow, and climate change. Water Resour. Res. 52, 813–826. https://doi.org/10.1002/2015WR017702.
Jackson, M.D., 2015. Tools and Techniques: self-potential methods. In: Schubert, G. (Ed.), 2nd ed. Treatise on Geophysics 11. Elsevier, Oxford, UK, pp. 261–293. https://doi.org/10.1016/B978-0-444-53802-4.00208-6.
Jacob, R.W., Hermance, J.F., 2004. Precision GPR measurements: assessing and compensating for instrument drift. In: Proceedings of the Tenth International Conference on Grounds Penetrating Radar. Delft, Netherlands, pp. 159–162.
JafarGandomi, A., Binley, A., 2013. A Bayesian trans-dimensional approach for the fusion of multiple geophysical datasets. J. Appl. Geophys. 96, 38–54. https://doi.org/10.1016/j.jappgeo.2013.06.004.
Jardani, A., Revil, A., Dupont, J.P., 2013. Advances in water resources stochastic joint inversion of hydrogeophysical data for salt tracer test monitoring and hydraulic conductivity imaging. Adv. Water Res. 52, 62–77. https://doi.org/10.1016/j.advwatres.2012.08.005.
Johnson, T.C., Versteeg, R.J., Hauang, H., Routh, P.S., 2009. Data-domain correlation approach for joint hydrogeologic inversion of time-lapse hydrogeologic and geophysical data. Geophysics 74 (6), F127–F140. http://library.seg.org/doi/abs/10.1190/1.3237087.
Johnson, T.C., Versteeg, R.J., Ward, A., Day-Lewis, F.D., Revil, A., 2010. Improved hydrogeophysical characterization and monitoring through parallel modeling and inversion of time-domain resistivity and induced-polarization data. Geophysics 75 (4), WA27–WA41.
Johnson, T.C., Slater, L.D., Ntarlagiannis, D., Day-Lewis, F.D., Elwaseif, M., 2012. Monitoring groundwater–surface water interaction using time-series and time-frequency analysis of transient three-dimensional electrical resistivity changes. Water Resour. Res. 48 (7), 1–12. W07506. https://doi.org/10.1029/2012WR011893.
Johnson, T.C., Rucker, D.F., Glaser, D.R., 2015. Near-surface geophysics at the Hanford nuclear site, the United States. In: Schubert, G. (Ed.), 2nd ed. Treatise on Geophysics 11. Elsevier, Oxford, UK, pp. 571–595. https://doi.org/10.1016/B978-0-444-53802-4.00205-0.
Jørgensen, F., Scheer, W., Thomsen, S., Sonnenborg, T.O., Hinsby, K., Wiederhold, H., Schamper, C., Burschil, T., Roth, B., Kirsch, R., Auken, E., 2012. Transboundary geophysical mapping of geological elements and salinity distribution critical for the assessment of future sea water intrusion in response to sea level rise. Hydrol. Earth Syst. Sci. 16 (7), 1845–1862. https://doi.org/10.5194/hess-16-1845-2012.
Kaika, M., 2003. The water framework directive: a new directive for a changing social, political and economic European framework. Eur. Plan. Stud. 11 (3), 299–316. https://doi.org/10.1080/0965431032000070802.
Kalbus, E., Reinstorf, F., Schirmer, M., 2006. Measuring methods for groundwater, surface water and their interactions: a review. Hydrol. Earth Syst. Sci. Discuss. 3 (4), 873–887. https://doi.org/10.5194/hessd-3-1809-2006.
Käser, D.H., Binley, A., Heathwaite, A.L., Krause, S., 2009. Spatio-temporal variations of hyporheic flow in a riffle-step-pool sequence. Hydrol. Processes 23 (15), 2138–2149. https://doi.org/10.1002/hyp.
Käser, D., Binley, A.M., Louise Heathwaite, A., 2013. On the importance of considering channel microforms in groundwater models of hyporheic exchange. River Res. Appl. 29 (4), 528–535. https://doi.org/10.1002/rra.
Kelly, B.F.J., Allen, D., Ye, K., Dahlin, T., 2009. Continuous electrical imaging for mapping aquifer recharge along reaches of the Namoi River in Australia. Near Surf. Geophys. 7 (4), 259–270.
Kemna, A., Binley, A., Slater, L., 2004. Crosshole IP imaging for engineering and environmental applications. Geophysics 69 (1), 97–107.
Kemna, A., Binley, A., Cassiani, G., Niederleithinger, E., Revil, A., Slater, L., Williams, K., Flores Orozco, A., Haegel, H., Kruschwitz, S., Leroux, V., Zimmermann, E., 2012. An overview of the spectral induced polarization method for near-surface applications. Near Surf. Geophys. 10, 453–468. https://doi.org/10.3997/1873-0604.2012027.
Kemna, A., Binley, A., Ramirez, A., Daily, W., 2000. Complex resistivity tomography for environmental applications. Chem. Eng. J. 77 (1), 11–18.
Kennedy, C.D., Genereux, D.P., Corbett, D.R., Mitasova, H., 2009. Relationships among groundwater age, denitrification, and the coupled groundwater and nitrogen fluxes through a streambed. Water Resour. Res. 45 (9), 1–15. W09402. https://doi.org/10.1029/2008WR007400.
Kiel, B.A., Cardenas, B.M., 2014. Lateral hyporheic exchange throughout the Mississippi River network. Nat. Geosci. 7, 413–417. https://doi.org/10.1038/ngeo2157.
King, J.N., Mehta, A.J., Dean, R.G., 2009. Generalized analytical model for benthic water flux forced by surface gravity waves. J. Geophys. Res. 114 (4), 1–14. C04004. https://doi.org/10.1029/2008JC005116.
Kinnear, J.A., Binley, A., Duque, C., Engesgaard, P.K., 2013. Using geophysics to map areas of potential groundwater discharge into Ringkøbing Fjord, Denmark. Lead. Edge 32 (7), 792–796.
Kirkegaard, C., Sonnenborg, T.O., Auken, E., Jørgensen, F., 2011. Salinity distribution in heterogeneous coastal aquifers mapped by airborne electromagnetics. Vadose Zone J. 10 (1), 125–135. https://doi.org/10.2136/vzj2010.0038.
Kowalsky, M.B., Finsterle, S., Peterson, J., Hubbard, S., Rubin, Y., Majer, E., Ward, A., Gee, G., 2005. Estimation of field-scale soil hydraulic and dielectric parameters through joint inversion of GPR and hydrological data. Water Resour. Res. 41 (11), 1–19. https://doi.org/10.1029/2005WR004237.
Kruse, S., 2013. Near-surface geophysics in geomorphology. In: Shroder, J., Bishop, M.P. (Eds.), Treatise on Geomorphology, Remote Sensing and GIScience in Geomorphology 3. Academic Press, California, US, pp. 103–129. https://doi.org/10.1016/B978-0-12-374739-6.00047-6.
Kuras, O., Pritchard, J.D., Meldrum, P.I., Chambers, J.E., Wilkinson, P.B., Ogilvy, R.D., Wealthall, G.P., 2009. Monitoring hydraulic processes with automated time-lapse electrical resistivity tomography (ALERT). C.R. Geosci. 341 (10–11), 868–885. https://doi.org/10.1016/j.crte.2009.07.010.
Lambot, S., Antoine, M., van den Bosch, I., Slob, E.C., Vanclooster, M., 2004. Electromagnetic inversion of GPR signals and subsequent hydrodynamic inversion to estimate effective vadose zone hydraulic properties. Vadose Zone J. 3 (4), 1072–1081. https://doi.org/10.2136/vzj2004.1072.
Lambot, S., Slob, E.C., Vanclooster, M., Vereecken, H., 2006. Closed loop GPR data

inversion for soil hydraulic and electric property determination. Geophys. Res. Lett. 33 (21), 4–5. L21405. https://doi.org/10.1029/2006GL027906.
Lansdown, K., Heppell, C.M., Trimmer, M., Binley, A., Heathwaite, A.L., Byrne, P., Zhang, H., 2015. The interplay between transport and reaction rates as controls on nitrate attenuation in permeable, streambed sediments. J. Geophys. Res.: Biogeosci. 120 (6), 1093–1109. https://doi.org/10.1002/2014JG002874.
Larsen, L.G., Harvey, J.W., Maglio, M.M., 2014. Dynamic hyporheic exchange at intermediate timescales: testing the relative importance of evapotranspiration and flood pulses minutes hours days weeks months years decades. Water Resour. Res. 50, 318–335. https://doi.org/10.1002/2013WR014195.
Lautz, L.K., Siegel, D.I., 2006. Modeling surface and ground water mixing in the hyporheic zone using MODFLOW and MT3D. Adv. Water Res. 29 (11), 1618–1633. https://doi.org/10.1016/j.advwatres.2005.12.003.
Lavoué, F., Van Der Kruk, J., Rings, J., André, F., Moghadas, D., Huisman, J.A., Lambot, S., Weihermüller, L., Vanderborght, J., Vereecken, H., 2010. Electromagnetic induction calibration using apparent electrical conductivity modelling based on electrical resistivity tomography. Near Surf. Geophys. 8 (6), 553–561.
Leroy, P., Revil, A., 2009. Spectral induced polarization of clays and clay-rocks. J. Geophys. Res. 11 (B10202), 1–21.
Lesmes, D.P., Frye, K.M., 2001. Influence of pore fluid chemistry on the complex conductivity and induced polarization responses of Berea sandstone. J. Geophys. Res.: Solid Earth 106 (B3), 4079–4090.
Lin, H., 2010. Earth's critical zone and hydropedology: concepts, characteristics, and advances. Hydrol. Earth Syst. Sci. 14, 25–45.
Linde, N., Binley, A., Tryggvason, A., Pedersen, L.B., Revil, A., 2006. Improved hydrogeophysical characterization using joint inversion of cross-hole electrical resistance and ground-penetrating radar traveltime data. Water Resour. Res. 42 (12), 1–16. W12404. https://doi.org/10.1029/2006WR005131.
Linde, N., Revil, A., 2007. Inverting self-potential data for redox potentials of contaminant plumes. Geophys. Res. Lett. 34 (14), 1–5. L14302. https://doi.org/10.1029/2007GL030084.
Linde, N., Renard, P., Mukerji, T., Caers, J., 2015. Geological realism in hydrogeological and geophysical inverse modeling: a review. Water Resour. Res. 86, 86–90.
Loheide, S.P., Lundquist, J.D., 2009. Snowmelt-induced diel fluxes through the hyporheic zone. Water Resour. Res. 45 (1), 1–9. https://doi.org/10.1029/2008WR007329.
Loke, M.H., Chambers, J.E., Rucker, D.F., Kuras, O., Wilkinson, P.B., 2013. Recent developments in the direct-current geoelectrical imaging method. J. Appl. Geophys. 95, 135–156. https://doi.org/10.1016/j.jappgeo.2013.02.017.
Loke, M.H., Wilkinson, P.B., Chambers, J.E., Uhlemann, S.S., Sorensen, J.P.R., 2015. Optimized arrays for 2-D resistivity survey lines with a large number of electrodes. J. Appl. Geophys. 112, 136–146. https://doi.org/10.1016/j.jappgeo.2014.11.011.
Malard, F., Tockner, K., Dole-Olivier, M., Ward, J.V., 2002. A landscape perspective of surface–subsurface hydrological exchanges in river corridors. Freshw. Biol. 47 (4), 621–640. https://doi.org/10.1046/j.1365-2427.2002.00906.x.
Malzone, J.M., Anseeuw, S.K., Lowry, C.S., Allen-King, R., 2016. Temporal hyporheic zone response to water table fluctuations. Groundwater 54 (2), 274–285. https://doi.org/10.1111/gwat.12352.
Mansoor, N., Slater, L., Artigas, F., Auken, E., 2006. High-resolution geophysical characterization of shallow-water wetlands. Geophysics 71 (4), B101–B109. https://doi.org/10.1190/1.2210307.
Mansoor, N., Slater, L., 2007. Aquatic electrical resistivity imaging of shallow-water wetlands. Geophysics 72 (5), F211–F221. https://doi.org/10.1190/1.2750667.
Marzadri, A., Tonina, D., Bellin, A., 2013a. Effects of stream morphodynamics on hyporheic zone thermal regime. Water Resour. Res. 49, 2287–2302. https://doi.org/10.1002/wrcr.20199.
Marzadri, A., Tonina, D., Bellin, A., 2013b. Quantifying the importance of daily stream water temperature fluctuations on the hyporheic thermal regime: Implication for dissolved oxygen dynamics. J. Hydrol. 507, 241–248. https://doi.org/10.1016/j.jhydrol.2013.10.030.
Marzadri, A., Dee, M.M., Tonina, D., Bellin, A., Tank, J.L., 2017. Role of surface and subsurface processes in scaling N_2O emissions along riverine networks. Proc. Natl. Acad. Sci. 114 (17), 4330–4335.
Meier, P., Kalscheuer, T., Podgorski, J.E., Kgotlhang, L., Green, A.G., Greenhalgh, S., Rabenstein, L., Doetsch, J., Kinzelbach, W., Auken, Esben, Mikkelsen, P., Foged, N., Jaba, B.C., Tshoso, G., Ntibinyane, O., 2014. Hydrogeophysical investigations in the western and north-central Okavango Delta (Botswana) based on helicopter and ground-based transient electromagnetic data and electrical resistance tomography. Geophysics 79 (5), B201–B211. https://doi.org/10.1190/geo2014-0001.1.
Menichino, G.T., Ward, A.S., Hester, E.T., 2014. Macropores as preferential flow paths in meander bends. Hydrol. Process. 28 (3), 482–495. https://doi.org/10.1002/hyp.9573.
Menichino, G.T., Hester, E.T., 2014. Hydraulic and thermal effects of in-stream structure-induced hyporheic exchange across a range of hydraulic conductivities. Water Resour. Res. 50, 4643–4661. https://doi.org/10.1002/2013WR014758.
Menke, W., 2012. Geophysical Data Analysis: Discrete Inverse Theory, 3rd ed. Elsevier, Massachusetts, US.
Mermillod-Blondin, F., Winiarski, T., Foulquier, A., Perrissin, A., Marmonier, P., 2015. Links between sediment structures and ecological processes in the hyporheic zone: ground-penetrating radar as a non-invasive tool to detect subsurface biologically active zones. Ecohydrology 8 (4), 626–641. https://doi.org/10.1002/eco.1530.
Michot, D., Benderitter, Y., Doringny, A., Nicoullaud, B., King, D., Tabbagh, A., 2003. Spatial and temporal monitoring of soil water content with an irrigated corn crop cover using surface electrical resistivity tomography. Water Resour. Res. 39 (5), 1–20. https://doi.org/10.1029/2002WR001581.
Miled, M.B.H., Miller, E.L., 2007. A projection-based level-set approach to enhance conductivity anomaly reconstruction in electrical resistance tomography. Inverse Problems 23 (6), 2375–2400. https://doi.org/10.1088/0266-5611/23/6/007.
Miller, R.B., Heeren, D.M., Fox, G.A., Halihan, T., Storm, D.E., Mittelstet, A.R., 2014. The hydraulic conductivity structure of gravel-dominated vadose zones within alluvial floodplains. J. Hydrol. 513, 229–240. https://doi.org/10.1016/j.jhydrol.2014.03.046.
Minsley, B., 2007. Modelling and Inversion of Self-Potential Data. Department of Earth, Atmospheric, and Planetary Sciences, Massachusetts Institute of Technology.
Montaron, B., 2009. Connectivity theory – a new approach to modeling non-archie rocks. Petrophysics 50 (2), 102–115.
Moysey, S., Singha, K., Knight, R., 2005. A framework for inferring field-scale rock physics relationships through numerical simulation. Geophys. Res. Lett. 32 (8), 1–4. https://doi.org/10.1029/2004GL022152.
Musgrave, D.L., Reeburgh, W.S., 1982. Density-driven interstitial water motion in sediments. Nature 299 (5881), 331–334.
Mwakanyamale, K., Slater, L., Binley, A., Ntarlagiannis, D., 2012. Lithologic imaging using complex conductivity: lessons learned from the Hanford 300 Area. Geophysics 77 (6), E397. https://doi.org/10.1190/geo2011-0407.1.
Nabighian, M.N., Macnae, J.C., 1991. Time-domain electromagnetic prospecting methods. In: Nabighian, M.N. (Ed.), Electromagnetic Methods in Applied Geophysics Theory 2. Society of Exploration Geophysicists, Oklahoma, US, pp. 427–520.
Nagorski, S.A., Moore, J.N., 1999. Arsenic mobilization in the hyporheic zone of a stream. Water Resour. Res. 35 (11), 3441–3450. https://doi.org/10.1029/1999WR900204.
Naudet, V., Revil, A., Bottero, J., Bégassat, P., 2003. Relationship between self-potential (SP) signals and redox conditions in contaminated groundwater. Geophys. Res. Lett. 30 (21), 1–4. https://doi.org/10.1029/2003GL018096.
Naudet, V., Revil, A., Rizzo, E., Bottero, J., Bégassat, P., 2004. Groundwater redox conditions and conductivity in a contaminant plume from geoelectrical investigations. Hydrol. Earth Syst. Sci. 8 (1), 8–22.
Nenna, V., Knight, R., 2013. Demonstration of a value of information metric to assess the use of geophysical data for a groundwater application. Geophysics 79 (1), E51–E60. https://doi.org/10.1190/geo2012-0474.1.
Newbold, J.D., O'Neill, R.V, Elwood, J.W., Van Winkle, W., 1982. Nutrient spiralling in streams: implications for nutrient limitation and invertebrate activity. Am. Nat. 120 (5), 628–652.
Newell, A.J., Sorensen, J.P.R., Chambers, J.E., Wilkinson, P.B., Uhlemann, S.S., Roberts, C., Gooddy, D.C., Vane, C.H., Binley, A., 2015. Fluvial response to late Pleistocene and Holocene environmental change in a Thames chalkland headwater: the Lambourn of southern England. Proc. Geol. Assoc. 126 (6), 683–697. https://doi.org/10.1016/j.pgeola.2015.08.008.
Nyquist, J.E., Freyer, P., Toran, L., 2008. Stream bottom resistivity tomography to map ground water discharge. Ground Water 46 (4), 561–569. https://doi.org/10.1111/j.1745-6584.2008.00432.x.
Ogilvy, R.D., Kuras, O., Meldrum, P.I., Wilkinson, P.B., Chambers, J.E, Sen, M., Gisbert, J., Jorreto, S., Frances, I., Pulido-Bosch, A., Tsourlos, P., 2009. Automated time-Lapse Electrical Resistivity Tomography (ALERT) for monitoring coastal aquifers. Near Surf. Geophys. 7 (5–6), 367–375.
Oldenborger, G.A., Logan, C.E., Hinton, M.J., Pugin, A.J.M., Sapia, V., Sharpe, D.R., Russell, H.A.J., 2016. Bedrock mapping of buried valley networks using seismic reflection and airborne electromagnetic data. J. Appl. Geophys. 128, 191–201. https://doi.org/10.1016/j.jappgeo.2016.03.006.
Oldenburg, D.W., Li, Y., 1999. Estimating depth of investigation in dc resistivity and IP surveys. Geophysics 64 (2), 403. https://doi.org/10.1190/1.1444545.
Packman, A.I., MacKay, J.S., 2003. Interplay of stream-subsurface exchange, clay particle deposition, and streambed evolution. Water Resour. Res. 39 (4), 1–10. https://doi.org/10.1029/2002WR001432.
Paine, J.G., 2003. Determining salinization extent, identifying salinity sources, and estimating chloride mass using surface, borehole, and airborne electromagnetic induction methods. Water Resour. Res. 39 (3), 1059. https://doi.org/10.1029/2001WR000710.
Parsekian, A.D., Comas, X., Slater, L., Glaser, P.H., 2011. Geophysical evidence for the lateral distribution of free phase gas at the peat basin scale in a large northern peatland. J. Geophys. Res.: Biogeosci. 116 (G03008), 1–14. https://doi.org/10.1029/2010JG001543.
Parsekian, A.D., Singha, K., Minsley, B.J., Holbrook, W.S., Slater, L., 2015. Multiscale geophysical imaging of the critical zone. Rev. Geophys. 53, 1–26. https://doi.org/10.1029/88EO01108.
Pastick, N.J., Jorgenson, M.T., Wylie, B.K., Minsley, B.J., Ji, L., Walvoord, M.A., Smith, B.D., Abraham, J.D., Rose, J.R., 2013. Extending airborne electromagnetic surveys for regional active layer and permafrost mapping with remote sensing and ancillary data, Yukon Flats Ecoregion, Central Alaska. Permafr. Periglac. Process. 24 (3), 184–199.
Phelps, G., Ippolito, C., Lee, R., Spritzer, J., Yeh, Y., 2014. Investigations into Near-real-time Surveying for Geophysical Data Collection Using an Autonomous Ground Vehicle. pp. 1–12 US Geological Survey Open File Report 2014-1013.
Pidlisecky, A., Singha, K., Day-Lewis, F.D., 2011. A distribution-based parametrization for improved tomographic imaging of solute plumes. Geophys. J. Int. 187 (1), 214–224. https://doi.org/10.1111/j.1365-246X.2011.05131.x.
Power, G., Brown, R.S., Imhof, J.G., 1999. Groundwater and fish–insights from northern North America. Hydrol. Process. 13 (3), 401–422.
Prendergast, L.J., Gavin, K., 2014. A review of bridge scour monitoring techniques. J. Rock Mech. Geotech. Eng. 6 (2), 138–149. https://doi.org/10.1016/j.jrmge.2014.01.007.
Refsgaard, J.C., Auken, E., Bamberg, C.A., Christensen, B.S.B., Clausen, T., Dalgaard, E., Effersø, F., Ernsten, V., Gertz, F., Hansen, A.L., He, X., Jacobsen, B.H., Jensen, K.H., Jørgensen, F., Jørgensen, L., F., Koch, J., Nilsson, B., Peterson, C., De Schepper, G., Schamper, C., Sørensen, K.I., Therrien, R., Thirup, C., Viezzoli, A., 2014. Science of

the total environment nitrate reduction in geologically heterogeneous catchments – a framework for assessing the scale of predictive capability of hydrological models. Sci. Total Environ. 468–469, 1278–1288. https://doi.org/10.1016/j.scitotenv.2013.07.042.
Revil, A., 2005. Self-potential signals associated with preferential ground water flow pathways in a buried paleo-channel. Geophys. Res. Lett. 32 (7), 1–4. L07401. https://doi.org/10.1029/2004GL022124.
Revil, A., Gevaudan, C., Lu, N., Maineult, A., 2008. Hysteresis of the self-potential response associated with harmonic pumping tests. Geophys. Res. Lett. 35 (16). L16402, 1–5. https://doi.org/10.1029/2008GL035025.
Revil, A., Mendonc, C.A., Atekwana, E.A., Kulessa, B., Hubbard, S.S., 2010. Understanding biogeobatteries: where geophysics meets microbiology. J. Geophys. Res. 115 (G00G02), 1–22. https://doi.org/10.1029/2009JG001065.
Revil, A., 2012. Spectral induced polarization of shaly sands: influence of the electrical double layer. Water Resour. Res. 48 (2), 1–23. https://doi.org/10.1029/2011WR011260.
Richards, L.A., Magnone, D., van Dongen, B.E., Polya, D.A., 2017. High resolution profile of inorganic aqueous geochemistry and key redox zones in an arsenic bearing aquifer in Cambodia. Sci. Total Environ. 590–591, 540–553. https://doi.org/10.1016/j.scitotenv.2017.02.217.
Rizzo, E., Suski, B., Revil, A., 2004. Self-potential signals associated with pumping tests experiments. J. Geophys. Res.: Solid Earth 109 (B10203), 1–14. https://doi.org/10.1029/2004JB003049.
Robinson, D.A., Abdu, H., Lebron, I., Jones, S.B., 2012. Imaging of hill-slope soil moisture wetting patterns in a semi-arid oak savanna catchment using time-lapse electromagnetic induction. J. Hydrol. 416–417, 39–49. https://doi.org/10.1016/j.jhydrol.2011.11.034.
Rosenberry, D.O., & LaBaugh, J.W. (2008). Field techniques for Estimating Water Fluxes Between Surface Water and Ground Water Techniques and Methods. US Geological Survey Techniques and Methods 4–D2, 1–128. http://pubs.usgs.gov/tm/04d02/.
Rubin, Y., Hubbard, S.S. (Eds.), 2005. Hydrogeophysics. Springer, Netherlands.
Sassen, D.S., Hubbard, S.S., Bea, S.A., Chen, J., Spycher, N., Denham, M.E., 2012. Reactive facies: an approach for parameterizing field-scale reactive transport models using geophysical methods. Water Resour. Res. 48 (10), 1–20. W10526. https://doi.org/10.1029/2011WR011047.
Sato, M., Mooney, H.M., 1960. The electrochemical mechanism of sulfide self-potentials. Geophysics 25 (1), 226–249. https://doi.org/10.1190/1.1438689.
Schmadel, N.M., Ward, A.S., Lowry, C.S., Malzone, J.M., 2016. Hyporheic exchange controlled by dynamic hydrologic boundary conditions. Geophys. Res. Lett. 43, 4408–4417. https://doi.org/10.1002/2016GL068286.
Schmitt, D.R., 2015. Geophysical properties of the near surface earth: seismic properties. In: Schubert, G. (Ed.), 2nd ed. Treatise on Geophysics 11. Elsevier, Oxford, UK, pp. 43–87.
Shanahan, P.W., Binley, A., Whalley, W.R., Watts, C.W., 2015. The use of electromagnetic induction to monitor changes in soil moisture profiles beneath different wheat genotypes. Soil Sci. Soc. Am. J. 79, 459–466.
Singha, K., Day-Lewis, F.D., Moysey, S., 2007. Accounting for tomographic resolution in estimating hydrologic properties from geophysical data. In: Hyndman, D.W., Day-Lewis, F.D., Singha, K. (Eds.), Subsurface Hydrology: Data Integration for Properties and Processes 171. American Geophysical Union, California, US, pp. 227–241. https://doi.org/10.1029/171GM16.
Singha, K., Pidlisecky, A., Day-Lewis, F.D., Gooseff, M.N., 2008. Electrical characterization of non-Fickian transport in groundwater and hyporheic systems. Water Resour. Res. 44 (4), 1–14. W00D07. https://doi.org/10.1029/2008WR007048.
Singha, K., Day-Lewis, F.D., Johnson, T., Slater, L.D., 2015. Advances in interpretation of subsurface processes with time-lapse electrical imaging. Hydrol. Process. 29 (6), 1549–1576. https://doi.org/10.1002/hyp.10280.
Slater, L.D., Binley, A., Brown, D., 1997. Electrical imaging of fractures using groundwater salinity change. Ground Water 35 (3), 436–442. https://doi.org/10.1111/j.1745-6584.1997.tb00103.x.
Slater, L., Lesmes, D.P., 2002. Electrical-hydraulic relationships observed for unconsolidated sediments. Water Resour. Res. 38 (10), 33–46. https://doi.org/10.1029/2001WR001075.
Slater, L., Binley, A., 2006. Synthetic and field-based electrical imaging of a zerovalent iron barrier: Implications for monitoring long-term barrier performance. Geophysics 71 (5), B129–B137. https://doi.org/10.1190/1.2235931.
Slater, L., 2007. Near surface electrical characterization of hydraulic conductivity: from petrophysical properties to aquifer geometries – a review. Surv. Geophys. 28 (2), 169–197. https://doi.org/10.1007/s10712-007-9022-y.
Slater, L., Ntarlagiannis, D., Yee, N., O'Brien, M., Zhang, C., Williams, K.H., 2008. Electrodic voltages in the presence of dissolved sulfide: implications for monitoring natural microbial activity. Geophysics 73 (2), F65–F70. http://doi.org/10.1190/1.2828977.
Slater, L.D., Ntarlagiannis, D., Day-Lewis, F.D., Mwakanyamale, K., Versteeg, R.J., Ward, A., Strickland, C., Johnson, C.D., Lane, J.W., 2010. Use of electrical imaging and distributed temperature sensing methods to characterize surface water-groundwater exchange regulating uranium transport at the Hanford 300 Area, Washington. Water Resour. Res. 46 (10), 5–13. W10533. https://doi.org/10.1029/2010WR009110.
Snyder, D.D., Wightman, W.E., 2002. Application of continuous resistivity profiling to aquifer characterization. In: Proceedings of the 15th Symposium on the Application of Geophysics to Engineering and Environmental Problems. Las Vegas, Nevada, USA Paper 13GSL10.
Sophocleous, M., 2002. Interactions between groundwater and surface water: the state of the science. Hydrogeol. J. 10 (1), 52–67. https://doi.org/10.1007/s10040-001-0170-8.
Soueid Ahmed, A., Jardani, A., Revil, A., Dupont, J.P., 2014. Hydraulic conductivity field characterization from the joint inversion of hydraulic heads and self-potential data. Water Resour. Res. 50, 3502–3522.
Soueid Ahmed, A., Jardani, A., Revil, A., Dupont, J.P., 2016. Joint inversion of hydraulic head and self-potential data associated with harmonic pumping tests. Water Resour. Res. 52 (9), 6769–6791.
Stanford, J.A., Ward, J.V., 1988. The hyporheic habitat of river ecosystems. Nature 335 (6185), 64–66. https://doi.org/10.1038/335064a0.
Stanford, J.A., Ward, J.V., 1993. An ecosystem perspective of alluvial rivers: connectivity and the hyporheic corridor. J. N. Am. Benthol. Soc. 12 (1), 48–60. https://doi.org/10.2307/1467685.
Steeples, D.W., 2005. Shallow seismic methods. In: Rubin, Y., Hubbard, S.S. (Eds.), Hydrogeophysics 2. Springer, Netherlands, pp. 215–251.
Stoll, J.B., 2013. Unmanned aircraft systems for rapid near surface geophysical measurements. International Archives of the Photogrammetry, Remote Sensing and Spatial Information Sciences. UAV-g2013, Rostock, Germany, pp. 391–394 XL-1/W2.
Stonedahl, S.H., Harvey, J.W., Wörman, A., Salehin, M., Packman, A.I., 2010. A multi-scale model for integrating hyporheic exchange from ripples to meanders. Water Resour. Res. 46 (12), 1–14. W12539. https://doi.org/10.1029/2009WR008865.
Stonedahl, S.H., Harvey, J.W., Packman, A.I., 2013. Interactions between hyporheic flow produced by stream meanders, bars, and dunes. Water Resour. Res. 49 (9), 5450–5461. https://doi.org/10.1002/wrcr.20400.
Stonestrom, D.A., & Constantz, J. (2003). Heat as a Tool for Studying the Movement of Ground Water Near Streams. US Geological Survey Circular 1260. p1–96. https://doi.org/SBN0-607-94071-9.
Swarzenski, P.W., Simonds, F.W., Paulson, T., Kruse, S., 2007. Geochemical and geophysical examination of submarine groundwater discharge and associated nutrient loading estimates into Lynch Cove, Hood Canal, WA. US Geol. Surv. Environ. Sci. Technol. 41 (20), 7022–7029. http://pubs.er.usgs.gov/publication/70031439.
Tarantola, A., 2005. Inverse Problem Theory and Methods for Model Parameter Estimation. US: Society for Industrial and Applied Mathematics, Philadelphia. https://doi.org/10.1137/1.9780898717921.
Telford, W.M., Geldart, R.E., Sheriff, R.E., 2010. Applied Geophysics, 2nd ed. Cambridge University Press, Cambridge, UK.
Terry, N., Day-Lewis, F.D., Robinson, J.L., Slater, L.D., Halford, K., Binley, A., Lane, J., Werkema, D., 2017. Scenario Evaluator for Electrical Resistivity Survey Pre-modeling Tool. Groundwater 6, 1–6. https://doi.org/10.1111/gwat.12522.
Tonina, D., Buffington, J.M., 2007. Hyporheic exchange in gravel bed rivers with pool-riffle morphology: laboratory experiments and three-dimensional modeling. Water Resour. Res. 43, 1–16. https://doi.org/10.1029/2005WR004328.
Tonina, D., Buffington, J.M., 2009. Hyporheic exchange in mountain rivers I: mechanics and environmental effects. Geogra. Compass 3 (3), 1063–1086.
Topp, G.C., Davis, J.L., & Annan, A.P. (1980). Electromagnetic determination of soil water content: Water Resour. Res., 16(3), 574–582. https://doi.org/10.1029/WR016i003p00574.
Toran, L., Hughes, B., Nyquist, J., Ryan, R., 2013b. Freeze core sampling to validate time-lapse resistivity monitoring of the hyporheic zone. Ground Water 51 (4), 635–640. https://doi.org/10.1111/j.1745-6584.2012.01002.x.
Toran, L., Hughes, B., Nyquist, J., Ryan, R., 2012. Using hydrogeophysics to monitor change in hyporheic flow around stream restoration structures. Environ. Eng. Geosci. 18 (1), 83–97. https://doi.org/10.2113/gseegeosci.18.1.83.
Toran, L., Nyquist, J.E., Fang, A.C., Ryan, R.J., Rosenberry, D.O., 2013a. Observing lingering hyporheic storage using electrical resistivity: variations around stream restoration structures, Crabby Creek, PA. Hydrol. Process. 27 (10), 1411–1425. https://doi.org/10.1002/hyp.9269.
Tóth, J., 1963. A theoretical analysis of groundwater flow in small drainage basins. J. Geophys. Res. 68 (16), 4795–4812.
Triska, F.J., Kennedy, V.C., Avanzino, R.J., Zellweger, G.W., Bencala, K.E., 1989. Retention and transport of nutrients in a third-order stream in Northwestern California: hyporheic processes. Ecology 70 (6), 1893–1905. http://www.jstor.org/stable/1938120.
Triska, F.J., Duff, J.H., Avanzino, R.J., 1993. The role of water exchange between a stream channel and its hyporheic zone in nitrogen cycling at the terrestrial aquatic interface. Hydrobiologia 251 (1–3), 167–184. https://doi.org/10.1007/BF00007177.
Tso, C.-H.M., Kuras, O., Wilkinson, P., Uhlemann, S., Chambers, J., Meldrum, P., Graham, J., Sherlock, E., Binley, A., 2017. Improved characterisation and modelling of measurement errors in electrical resistivity tomography (ERT) surveys. Advance online publication. https://doi.org/10.1016/j.jappgeo.2017.09.009.
Uhlemann, S.S., Sorensen, J.P.R., House, A.R., Wilkinson, P.B., Roberts, C., Gooddy, D.C., Binley, A.M., Chambers, J.E., 2016. Integrated time-lapse geoelectrical imaging of wetland hydrological processes. Water Resour. Res. 52 (3), 1607–1625. https://doi.org/10.1002/2015WR017932.
Uhlemann, S., Kuras, O., Richards, L.A., Naden, E., Polya, D.A., 2017. Electrical resistivity tomography determines the spatial distribution of clay layer thickness and aquifer vulnerability, Kandal Province, Cambodia. J. Asian Earth Sci Advance online publication. https://doi.org/10.1016/j.jseaes.2017.07.043.
Valett, H.M., Hakenkamp, C.C., Boulton, A.J., 1993. Perspectives on the hyporheic zone: integrating hydrology and biology. J. N. Am. Benthol. Soc. 12 (1), 40–43 http://www.jstor.org/stable/1467683 12.
van der Kruk, J., 2015. Tools and techniques: ground-penetrating radar. In: Schubert, G. (Ed.), 2nd ed. Treatise on Geophysics 11. Elsevier, Oxford, UK, pp. 209–232. https://doi.org/10.1016/B978-0-444-53802-4.00195-0.
Viezzoli, A., Tosi, L., Teatini, P., Silvestri, S., 2010. Surface water-groundwater exchange in transitional coastal environments by airborne electromagnetics: the Venice Lagoon example. Geophys. Res. Lett. 37 (1), 1–6. L01402. https://doi.org/10.1029/2009GL041572.
Vinegar, H.J., Waxman, M.H., 1984. Induced polarization of shaly sands. Geophysics 49

(8), 1267–1287. https://doi.org/10.1190/1.1441755.
Von Gunten, H.R., Karametaxas, G., Krähenbühl, U., Kuslys, M., Giovanoli, R., Hoehn, E., Keil, R., 1991. Seasonal biogeochemical cycles in riverborne groundwater. Geochimica et Cosmochimica Acta 55, 3597–3609.
Voytek, E.B., Rushlow, C.R., Godsey, S.E., Singha, K., Science, H., Program, E., Engineering, G., 2016. Identifying hydrologic flowpaths on arctic hillslopes using electrical resistivity and self-potential. Geophysics 81 (1), 1–31. https://doi.org/10.1190/GEO2015-0172.1.
Wallin, E.L., Johnson, T.C., Greenwood, W.J., Zachara, J.M., 2013. Imaging high stage river-water intrusion into a contaminated aquifer along a major river corridor using 2-D time-lapse surface electrical resistivity tomography. Water Resour. Res. 49 (3), 1693–1708. https://doi.org/10.1002/wrcr.20119.
Ward, A.S., Singha, K., Gooseff, M.N., 2010a. Imaging hyporheic zone solute transport using electrical resistivity. Hydrol. Process. 24 (7), 948–953. https://doi.org/10.1002/hyp.7672.
Ward, A.S., Gooseff, M.N., Singha, K., 2010b. Characterizing hyporheic transport processes – interpretation of electrical geophysical data in coupled stream-hyporheic zone systems during solute tracer studies. Adv. Water Res. 33 (11), 1320–1330. https://doi.org/10.1016/j.advwatres.2010.05.008.
Ward, A.S., Gooseff, M.N., Singha, K., 2013. How does subsurface characterization affect simulations of hyporheic exchange? Ground Water 51 (1), 14–28. https://doi.org/10.1111/j.1745-6584.2012.00911.x.
Ward, A.S., 2016. The evolution and state of interdisciplinary hyporheic research. Wiley Interdiscip. Rev.: Water. pp. 83–103. https://doi.org/10.1002/wat2.1120.
Waxman, M.H., Smits, L.J.M., 1968. Electrical conductivities in oil-bearing shaly sands. Soc. Pet. Eng. Trans. 243, 107–122. https://doi.org/10.2118/1863-A.
Webb, D.J., Anderson, N.L., Newton, T., Cardimona, S., 2000. Bridge Scour: Application of Ground Penetrating Radar. Federal Highway Administration and Missouri Department of Transportation, pp. 1–19 Special Publication.
Webster, I.T., Norquay, S.J., Ross, F.C., Wooding, R.A., 1996. Solute exchange by convection within estuarine sediments. Estuar. Coast. Shelf Sci. 42 (2), 171–183. https://doi.org/10.1006/ecss.1996.0013.
Weller, A., Slater, L., Nordsiek, S., 2013. On the relationship between induced polarization and surface conductivity: implications for petrophysical interpretation of electrical measurements. Geophysics 78 (5), D315–D325. https://doi.org/10.1190/geo2013-0076.1.
Weller, A., Slater, L., Binley, A., Nordsiek, S., Xu, S., 2015a. Permeability prediction based on induced polarization: insights from measurements on sandstone and unconsolidated samples spanning a wide permeability range. Geophysics 80 (2), D161–D173. https://doi.org/10.1190/geo2014-0368.1.
Weller, A., Slater, L., Huisman, J.A., Esser, O., Haegel, F., 2015b. On the specific polarizability of sands and sand-clay mixtures. Geophysics 80 (3), A57–A61. https://doi.org/10.1190/GEO2014-0509.1.
Weller, A., Slater, L.D., 2015. Induced polarization dependence on pore space geometry: empirical observations and mechanistic predictions. J. Appl. Geophys. 123, 310–315. https://doi.org/10.1016/j.jappgeo.2015.09.002.
Whitehead, K., Hudenholtz, C.H., 2014a. Remote sensing of the environment with small unmanned aircraft systems (UASs) part 1: a review of progress and challenges. J. Unmanned Veh. Syst. 2 (3), 69–85.
Whitehead, K., Hugenholtz, C.H., Myshak, S., Brown, O., LeClair, A., Tamminga, A., Barchyn, T.E., Moorman, B., Eaton, B., 2014b. Remote sensing of the environment with small unmanned aircraft systems (UASs) part 2: scientific and commercial applications. J. Unmanned Veh. Syst. 2 (3), 86–102.
Wilkinson, P.B., Meldrum, P.I., Chambers, J.E., Kuras, O., Ogilvy, R., 2006. Improved strategies for the automatic selection of optimized sets of electrical resistivity tomography measurement configurations. Geophys. J. Int. 167 (3), 1119–1126.
Wilkinson, P.B., Meldrum, P.I., Kuras, O., Chambers, J.E., Holyoake, S.J., Ogilvy, R.D., 2010. High-resolution electrical resistivity tomography monitoring of a tracer test in a confined aquifer. J. Appl. Geophys. 70 (4), 268–276. https://doi.org/10.1016/j.jappgeo.2009.08.001.
Wilkinson, P.B., Loke, M.H., Meldrum, P.I., Chambers, J.E., Kuras, O., Gunn, D.A., Ogilvy, R.D., 2012. Practical Aspects of Applied Optimised Survey Design for Electrical Resistivity Tomography. https://doi.org/10.1111/j.1365-246X.2012.05372.x/pdf.
Williams, B.A., Thompson, M.D., Miller, S.F., 2012a. Integrated Surface Geophysical Investigation Results at Liquid Effluent Retention Facility, 200 East Area, Hanford. CH2MHill Plateau Remediation Company, , Washington.
Williams, B.A., Thompson, M.D., Miller, S.F., 2012b. Interpretation and Integration of Seismic Data in the Gable Gap. CH2MHill Plateau Remediation Company.
Williams, B.A., Thompson, M.D., Miller, S.F., 2012c. Land Streamer and Gimbaled Geophones Phase II-200 Areas: High-Resolution Seismic Reflection Survey At the Hanford Site. CH2MHill Plateau Remediation Company.
Williams, B.A., Thompson, M.D., Miller, S.F., 2012d. Seismic Reflection Investigation At the Liquid Effluent Retention Facility, 200 East Area, Hanford Site. CH2MHill Plateau Remediation Company, Richland, Washington.
Williams, K.H., Ntarlagiannis, D., Slater, L.D., Dohnalkova, A., Hubbard, S.S., Banfield, J.F., 2005. Geophysical imaging of stimulated microbial biomineralization. Environ. Sci. Technol. 39 (19), 7592–7600. http://doi.org/10.1021/es0504035.
Wilson, J., Coxon, C., Rocha, C., 2016. A GIS and remote sensing based screening tool for assessing the potential for groundwater discharge to lakes in Ireland. Biol. Environ.: Proc. R. Irish Acad. 116B (3), 265–277. https://doi.org/10.3318/bioe.2016.15.
Winter, T. (1976). Numerical Simulation Analysis of the Interaction of Lakes and Groundwater. US Geological Survey Professional Paper 1001, 1–45. https://pubs.er.usgs.gov/publication/pp1001.
Winter, T.C., Harvey, J.W., Franke, O.L., & Alley, W.M. (1998). Ground Water and Surface Water: A Single Resource. US Geological Survey Circular 1139, 1–79.
Wishart, D.N., Slater, L.D., Gates, A.E., 2006. Self-potential improves characterization of hydraulically-active fractures from azimuthal geoelectrical measurements. Geophys. Res. Lett. 33 (17), 2–6. https://doi.org/10.1029/2006GL027092.
Wishart, D.N., Slater, L.D., Gates, A.E., 2008. Fracture anisotropy characterization in crystalline bedrock using field-scale azimuthal self-potential gradient. J. Hydrol. 358 (1–2), 35–45. https://doi.org/10.1016/j.jhydrol.2008.05.017.
Woessner, W.W., 2000. Stream and fluvial plain ground water interactions: rescaling hydrogeological thought. Ground Water 38 (3), 423–429.
Wojnar, A.J., Mutiti, S., Levy, J., 2013. Assessment of geophysical surveys as a tool to estimate riverbed hydraulic conductivity. J. Hydrol. 482, 40–56. https://doi.org/10.1016/j.jhydrol.2012.12.018.
Wondzell, S.M., Gooseff, M.N., McGlynn, B.L., 2010. An analysis of alternative conceptual models relating hyporheic exchange flow to diel fluctuations in discharge during baseflow recession. Hydrol. Process. 24 (6), 686–694. https://doi.org/10.1002/hyp.7507.
Worrall, L., Munday, T.J., Green, A.A., 1999. Airborne electromagnetics – providing new perspectives on geomorphic process and landscape development in regolith-dominated terrains. Phys. Chem. Earth 24 (10), 855–860. https://doi.org/10.1016/S1464-1895(99)00127-1.
Wynn, J.C., Sherwood, S.I., 1986. The self-potential (SP) method: an inexpensive reconnaissance and archaeological mapping tool. J. Field Archaeol. 11 (2), 195–204. https://doi.org/10.1179/jfa.1984.11.2.195.
Xie, Y., Cook, P.G., Shanafield, M., Simmons, C.T., Zheng, C., 2016. Uncertainty of natural tracer methods for quantifying river-aquifer interaction in a large river. J. Hydrol. 535, 135–147. https://doi.org/10.1016/j.jhydrol.2016.01.071.
Yoshikawa, K., Hinzman, L.D., 2003. Shrinking thermokarst ponds and groundwater dynamics in discontinuous permafrost near Council, Alaska. Permafr. Periglac. Process. 14 (2), 151–160. https://doi.org/10.1002/ppp.451.
Zarroca, M., Linares, R., Rodellas, V., Garcia-Orellana, J., Roqué, C., Bach, J., Masqué, P., 2014. Delineating coastal groundwater discharge processes in a wetland area by means of electrical resistivity imaging, 224Ra and 222Rn. Hydrol. Process. 28 (4), 2382–2395. https://doi.org/10.1002/hyp.9793.
Zhang, J., Revil, A., 2015. 2D joint inversion of geophysical data using petrophysical clustering and facies deformation. Geophysics 80 (5), M69–M88. https://doi.org/10.1190/geo2015-0147.1.
Zhou, B., Greenhalgh, S.A., 2000. Cross-hole resistivity tomography using different electrode configurations. Geophys. Prospect. 48 (5), 887–912. https://doi.org/10.1046/j.1365-2478.2000.00220.x.
Zhou, J., Revil, A., Karaoulis, M., Hale, D., Doetsch, J., Cuttler, S., 2014. Image-guided inversion of electrical resistivity data. Geophys. J. Int. 197 (1), 292–309. https://doi.org/10.1093/gji/ggu001.
Zimmer, M.A., Lautz, L.K., 2014. Temporal and spatial response of hyporheic zone geochemistry to a storm event. Hydrol. Process. 28 (4), 2324–2337. https://doi.org/10.1002/hyp.9778.